A ROBUST FINITE ELEMENT METHOD FOR DARCY–STOKES FLOW

KENT ANDRE MARDAL, XUE–CHENG TAI, AND RAGNAR WINTHER

Abstract. Finite element methods for a family of systems of singular perturbation problems of a saddle point structure are discussed. The system is approximately a linear Stokes problem when the perturbation parameter is large, while it degenerates to a mixed formulation of Poisson's equation as the perturbation parameter tends to zero. It is established, basically by numerical experiments, that most of the proposed finite element methods for Stokes problem or the mixed Poisson's system are not well behaved uniformly in the perturbation parameter. This is used as the motivation for introducing a new "robust" finite element which exhibits this property.

1. Introduction

Let $\Omega \subset \mathbb{R}^2$ be a bounded and connected polygonal domain with boundary $\partial\Omega$. In this paper we shall consider finite element methods for the following singular perturbation problem:

$$\begin{aligned} (\boldsymbol{I} - \varepsilon^2 \boldsymbol{\Delta})\boldsymbol{u} - \mathbf{grad}\, p &= \boldsymbol{f} \quad \text{in } \Omega, \\ \operatorname{div} \boldsymbol{u} &= g \quad \text{in } \Omega, \\ \boldsymbol{u} &= 0 \quad \text{on } \partial\Omega. \end{aligned} \tag{1.1}$$

Here $\varepsilon \in (0, 1]$ is a parameter, while $\boldsymbol{\Delta} = \mathbf{diag}(\Delta, \Delta)$ is the Laplace operator on vector fields. The vector field $\boldsymbol{f}$ and scalar field g represent the data. The problem (1.1) only admits a solution if the function g has mean value zero on Ω and "the pressure" p is only determined up to addition of a constant.

We note that when ε is not too small, and $g = 0$, this problem is simply a standard Stokes problem, but with an additional non–harmful lower order term. However, if $\boldsymbol{f} = 0$ and ε approaches zero then the model problem formally tends to a mixed formulation of the Poisson equation with homogeneous Neumann boundary conditions.

When $\varepsilon = 0$ the first equation in (1.1) has the form of Darcy's law for flow in a homogeneous porous medium, where $\boldsymbol{u}$ is a volume averaged velocity. In fact, the system (1.1) can be regarded as a macroscopic

1991 *Mathematics Subject Classification.* Primary 65N12, 65N15, 65N30.

Key words and phrases. singular perturbation problems, Darcy–Stokes flow, nonconforming finite elements, uniform error estimates.

This work was partially supported by the Research Council of Norway (NFR), under grants 128224/431, 133755/441, and 135420/431.

model for flow in an "almost porous media," where $\boldsymbol{u}$ and p represents volume averaged velocity and pressure, respectively. The zero order velocity term in the first equation of (1.1) then typically represents a *Stokes drag*. An attempt to derive Darcy's law from volume averaged Stokes flow is for example discussed in [16]. Generalizations of the system (1.1) have also been proposed in the modeling of macrosegregation formation in binary alloy solidification, cf. [13]. Systems of the form (1.1) may also arise from time discretizations of the Navier–Stokes equation, where the parameter ε corresponds to the square root of the time step, cf. [3]. However, the study of such time discretizations is not the motivation for the present paper.

The purpose of the present paper is to discuss a finite element method for the model problem (1.1) with convergence properties that are uniform with respect to the perturbation parameter ε. In §2 we will introduce some notations and discuss various properties of the model (1.1). Discretizations of the model problem by the finite element method is described in §3. In particular, we will state stability conditions which are uniform with respect to the parameter ε, and show, by numerical experiments, that the standard discretizations, proposed either for $\varepsilon = 1$ or $\varepsilon = 0$, do not satisfy these stability conditions. A new nonconforming finite element discretization is then proposed in §4. We show that this new discretization is uniformly stable, and, as a consequence we establish, in §5, error estimates which are uniform in ε under the assumption that proper regularity estimates hold for the solution. In §6 we then study the asymptotic smoothness of the solution of (1.1) as ε tends to zero. Based on these regularity results we show that, for fixed data $\boldsymbol{f}$ and g, a uniform $O(h^{1/2})$ error estimate in a suitable energy norm can be derived.

In the final section of this paper we study an elliptic system which formally is a generalization of (1.1). This system is given by

$$\begin{aligned} (\boldsymbol{I} - \varepsilon^2 \boldsymbol{\Delta})\boldsymbol{u} - \delta^{-2}\,\mathbf{grad}(\operatorname{div} \boldsymbol{u} - g) &= \boldsymbol{f} \quad \text{in } \Omega, \\ \boldsymbol{u} &= 0 \quad \text{on } \partial\Omega, \end{aligned} \tag{1.2}$$

where $\varepsilon, \delta \in (0, 1]$. By introducing $p = \delta^{-2}(\operatorname{div} \boldsymbol{u} - g)$ this system can be alternatively written on the mixed form

$$\begin{aligned} (\boldsymbol{I} - \varepsilon^2 \boldsymbol{\Delta})\boldsymbol{u} - \mathbf{grad}\, p &= \boldsymbol{f} \quad \text{in } \Omega, \\ \operatorname{div} \boldsymbol{u} - \delta^2 p &= g \quad \text{in } \Omega, \\ \boldsymbol{u} &= 0 \quad \text{on } \partial\Omega. \end{aligned} \tag{1.3}$$

Note that this system also has meaning when $\delta = 0$, and in this case the system reduces to (1.1).

The symmetric and positive definite system (1.2) is discretized by a straightforward finite element approach utilizing the new nonconforming velocity space constructed earlier in this paper, i.e. the mixed

system (1.3) is not introduced in the discretization. We show, by numerical experiments and theory, that under the assumption of sufficiently regular solutions, we obtain error estimates which are uniform both in ε and δ.

2. Preliminaries

We will use $H^m = H^m(\Omega)$ to denote the Sobolev space of scalar functions on Ω with m derivatives in $L^2 = L^2(\Omega)$, with norm $\|\cdot\|_m$. Furthermore, the notation $\|\cdot\|_{m,K}$ is used to indicate that the norm is defined with respect to a domain K different from Ω. The seminorm derived from the partial derivatives of order equal m is denoted $|\cdot|_m$, i.e. $|\cdot|_m^2 = \|\cdot\|_m^2 - \|\cdot\|_{m-1}^2$. The space $H_0^m = H_0^m(\Omega)$ will denote the closure in H^m of $C_0^\infty(\Omega)$. The dual space of H_0^m with respect to the L^2 inner product will be denoted by H^{-m}. Furthermore, L_0^2 will denote the space of L^2 functions with mean value zero. A space written in boldface denotes a 2–vector valued analog of the corresponding scalar space. The notation $(\cdot,\cdot)$ is used to denote the L^2 inner product on scalar, vector, and matrix valued functions.

Below we shall encounter the intersection and sum of Hilbert spaces. We therefore recall the basic definitions of these concepts. If X and Y are Hilbert spaces, both continuously contained in some larger Hilbert spaces, then the intersection $X \cap Y$ and the sum $X + Y$ are themselves Hilbert spaces with the norms

$$\|z\|_{X\cap Y} = (\|z\|_X^2 + \|z\|_Y^2)^{1/2}$$

and

$$\|z\|_{X+Y} = \inf_{\substack{z=x+y\\ x\in X,\, y\in Y}} (\|x\|_X^2 + \|y\|_Y^2)^{1/2}.$$

Furthermore, if $X \cap Y$ is dense in both X and Y then $(X \cap Y)^* = X^* + Y^*$. We refer to [4, Chapter 2] for these results.

If q is a scalar field then $\mathbf{grad}\, q$ will denote the gradient of q, while $\operatorname{div} \boldsymbol{v}$ denotes the divergence of a vector field $\boldsymbol{v}$. We shall also use the diffential operators

$$\mathbf{curl}\, q = \begin{pmatrix} -\partial q/\partial x_2 \\ \partial q/\partial x_1 \end{pmatrix} \quad \text{and} \quad \operatorname{rot} \boldsymbol{v} = \partial \boldsymbol{v}_1/\partial x_2 - \partial \boldsymbol{v}_2/\partial x_1.$$

Note that, due to Green's theorem, these definitions lead to the following "integration by parts formula"

$$\int_\Omega \mathbf{curl}\, q \cdot \boldsymbol{v}\, dx = \int_\Omega q \operatorname{rot} \boldsymbol{v}\, dx + \int_{\partial\Omega} q(\boldsymbol{v}\cdot\boldsymbol{t})\, d\tau, \tag{2.1}$$

where $\boldsymbol{t}$ is the unit tangent vector in the counter clockwise direction on $\partial\Omega$, and τ is the arclength.

The gradient of a vector field $\boldsymbol{v}$ is denoted $\boldsymbol{Dv}$, i.e. $\boldsymbol{Dv}$ is the 2×2 matrix with elements

$$(\boldsymbol{Dv})_{i,j} = \partial \boldsymbol{v}_i / \partial x_j \quad 1 \leq i, j \leq 2.$$

Hence, for any $\boldsymbol{u} \in \boldsymbol{H}^2$ and $\boldsymbol{v} \in \boldsymbol{H}_0^1$ we have

$$-(\boldsymbol{\Delta u}, \boldsymbol{v}) = (\boldsymbol{Du}, \boldsymbol{Dv}) \equiv \int_\Omega \boldsymbol{Du} : \boldsymbol{Dv}\, dx,$$

where the colon denotes the scalar product of matrix fields. Recall also the identity

$$\boldsymbol{\Delta} = \mathbf{grad}\,\mathrm{div} - \mathbf{curl}\,\mathrm{rot}, \tag{2.2}$$

which can be verified by a direct computation. As a consequence, we obtain the identity

$$(\boldsymbol{Du}, \boldsymbol{Dv}) = (\mathrm{div}\,\boldsymbol{u}, \mathrm{div}\,\boldsymbol{v}) + (\mathrm{rot}\,\boldsymbol{u}, \mathrm{rot}\,\boldsymbol{v}) \quad \forall \boldsymbol{u} \in \boldsymbol{H}^1,\ \boldsymbol{v} \in \boldsymbol{H}_0^1. \tag{2.3}$$

In addition to the function spaces introduced above we will also use the space $\boldsymbol{H}(\mathrm{div}) = \boldsymbol{H}(\mathrm{div}; \Omega)$ consisting of all vector fields in $\boldsymbol{L}^2$ with divergence in L^2, i.e.

$$\boldsymbol{H}(\mathrm{div}) = \{\boldsymbol{v} \in \boldsymbol{L}^2 : \mathrm{div}\,\boldsymbol{v} \in L^2\}.$$

Similarly,

$$\boldsymbol{H}(\mathrm{rot}) = \{\boldsymbol{v} \in \boldsymbol{L}^2 : \mathrm{rot}\,\boldsymbol{v} \in L^2\},$$

and the norms of these spaces are denoted by $\|\cdot\|_{\mathrm{div}}$ and $\|\cdot\|_{\mathrm{rot}}$, respectively. Furthermore, $\boldsymbol{H}_0(\mathrm{div})$ is the closed subspace of $\boldsymbol{H}(\mathrm{div})$ consisting of functions with vanishing normal component on the boundary, i.e.

$$\boldsymbol{H}_0(\mathrm{div}) = \{\boldsymbol{v} \in \boldsymbol{H}(\mathrm{div}) : \boldsymbol{v} \cdot \boldsymbol{n} = 0 \quad \text{on } \partial\Omega\},$$

where $\boldsymbol{n}$ is the unit outward normal vector.

Throughout this paper $a_\varepsilon(\cdot, \cdot) : \boldsymbol{H}^1 \times \boldsymbol{H}^1 \mapsto \mathbb{R}$ will denote the bilinear form

$$a_\varepsilon(\boldsymbol{u}, \boldsymbol{v}) = (\boldsymbol{u}, \boldsymbol{v}) + \varepsilon^2 (\boldsymbol{Du}, \boldsymbol{Dv}).$$

A weak formulation of problem (1.1) is given by:

Find $(\boldsymbol{u}, p) \in \boldsymbol{H}_0^1 \times L_0^2$ such that

$$\begin{aligned} a_\varepsilon(\boldsymbol{u}, \boldsymbol{v}) + (p, \mathrm{div}\,\boldsymbol{v}) &= (\boldsymbol{f}, \boldsymbol{v}) \qquad \forall \boldsymbol{v} \in \boldsymbol{H}_0^1, \\ (\mathrm{div}\,\boldsymbol{u}, q) &= (g, q) \qquad \forall q \in L_0^2. \end{aligned} \tag{2.4}$$

Here we assume that data $(\boldsymbol{f}, g)$ is given in $\boldsymbol{H}^{-1} \times L_0^2$.

The problem (2.4) has a unique solution $(\boldsymbol{u}, p) \in \boldsymbol{H}_0^1 \times L_0^2$. This follows from standard results for Stokes problem, cf. for example [11]. However, the bound on $(\boldsymbol{u}, p) \in \boldsymbol{H}_0^1 \times L_0^2$ will degenerate as ε tends to zero. In fact, for the reduced problem (2.4) with $\varepsilon = 0$ the space $\boldsymbol{H}_0^1 \times L_0^2$ is not a proper function space for the solution. However, the theory developed in [6] can be applied in this case if we seek $(\boldsymbol{u}, p)$ either in $\boldsymbol{H}_0(\mathrm{div}) \times L_0^2$ or in $\boldsymbol{L}^2 \times (H^1 \cap L_0^2)$, and with data $(\boldsymbol{f}, g)$ in the

proper dual spaces. These results are in fact consequences of standard results for the Poisson equation.

The fact that the regularity of the solution is changed when ε becomes zero strongly suggests that ε–dependent norms and function spaces are required in order to obtain stability estimates independent of ε. Furthermore, since the reduced problem is well posed for two completely different choices of function spaces, this indicates that there are at least two different choices of ε–dependent norms. In present paper we will study the problem (1.1) with respect to an ε–dependent norm which reduces to the norm in $\boldsymbol{H}_0(\mathrm{div}) \times L^2_0$ when $\varepsilon = 0$. Our goal is to derive discretizations which are uniformly stable with respect to ε in this norm. This appears to be the proper choice if we want to study discretizations which also can be generalized to non-mixed approximations of elliptic problems of the form (1.2).

Remark. When we refer to the *reduced system* corresponding to (1.1) we refer to the system (1.1) with $\varepsilon = 0$ and the boundary condition $\boldsymbol{u} = 0$ replaced by $\boldsymbol{u} \cdot \boldsymbol{n} = 0$. This system has a weak formulation given by (2.4), but with the solution space $\boldsymbol{H}^1_0$ replaced by $\boldsymbol{H}_0(\mathrm{div})$. □

The space $\boldsymbol{H}_0(\mathrm{div}) \cap \varepsilon \cdot \boldsymbol{H}^1_0$, with norm $|\!|\!| \cdot |\!|\!|_\varepsilon$ given by

$$|\!|\!| \boldsymbol{v} |\!|\!|^2_\varepsilon = \|\boldsymbol{v}\|^2_0 + \|\operatorname{div} \boldsymbol{v}\|^2_0 + \varepsilon^2 \|\boldsymbol{D}\boldsymbol{v}\|^2_0,$$

is equal to $\boldsymbol{H}^1_0$ as a set for $\varepsilon > 0$, but equal to $\boldsymbol{H}_0(\mathrm{div})$ for $\varepsilon = 0$. The system (2.4) can alternatively be written as the system

$$\mathcal{A}_\varepsilon \begin{pmatrix} \boldsymbol{u} \\ p \end{pmatrix} = \begin{pmatrix} \boldsymbol{f} \\ g \end{pmatrix},$$

where the coefficient operator $\mathcal{A}_\varepsilon$ is given by

$$\mathcal{A}_\varepsilon = \begin{pmatrix} \boldsymbol{I} - \varepsilon^2 \boldsymbol{\Delta} & -\mathbf{grad} \\ \mathrm{div} & 0 \end{pmatrix}. \tag{2.5}$$

Let $\boldsymbol{X}_\varepsilon$ be the product space $(\boldsymbol{H}_0(\mathrm{div}) \cap \varepsilon \cdot \boldsymbol{H}^1_0) \times L^2_0$ and $\boldsymbol{X}^*_\varepsilon$ the corresponding dual space with respect to the L^2–inner product. This space can also be expressed as

$$\boldsymbol{X}^*_\varepsilon = (\boldsymbol{H}^{-1}(\mathrm{rot}) + \varepsilon^{-1} \boldsymbol{H}^{-1}) \times L^2_0.$$

Here the + sign has the interpretation as the sum of Hilbert spaces, and the space $\boldsymbol{H}^{-1}(\mathrm{rot})$ is given by

$$\boldsymbol{H}^{-1}(\mathrm{rot}) = \{\boldsymbol{v} \in \boldsymbol{H}^{-1} : \mathrm{rot}\, \boldsymbol{v} \in H^{-1}\}.$$

The operator $\mathcal{A}_\varepsilon$ can be seen to be an isomorphism mapping $\boldsymbol{X}_\varepsilon$ into $\boldsymbol{X}^*_\varepsilon$. Furthermore, the corresponding operator norms

$$||\mathcal{A}_\varepsilon||_{\mathcal{L}(X_\varepsilon, X^*_\varepsilon)} \quad \text{and} \quad ||\mathcal{A}^{-1}_\varepsilon||_{\mathcal{L}(X^*_\varepsilon, X_\varepsilon)}$$

are independent of ε. In fact, with the definitions above, this is also true for $\varepsilon \in [0, 1]$, i.e. the endpoint $\varepsilon = 0$ can be included.

The uniform boundedness of $\mathcal{A}_\varepsilon$ is straightforward to check from the definitions above, while the uniform boundedness of the inverse can be

verified from the two Brezzi conditions, cf. [6]. For the present problem these conditions read:

There are constants $\alpha_0, \beta_0 > 0$, independent of ε, such that

$$\sup_{\boldsymbol{v}\in \boldsymbol{H}_0(\mathrm{div})\cap \varepsilon\cdot \boldsymbol{H}_0^1} \frac{(q, \mathrm{div}\, \boldsymbol{v})}{|\!|\!| \boldsymbol{v} |\!|\!|_\varepsilon} \geq \alpha_0 \|q\|_0 \quad \forall q \in L_0^2, \tag{2.6}$$

and

$$a_\varepsilon(\boldsymbol{v}, \boldsymbol{v}) \geq \beta_0 |\!|\!| \boldsymbol{v} |\!|\!|_\varepsilon^2 \quad \forall \boldsymbol{v} \in \boldsymbol{Z}, \tag{2.7}$$

where $\boldsymbol{Z} = \{\boldsymbol{v} \in \boldsymbol{H}_0^1 : \mathrm{div}\, \boldsymbol{v} = 0\}$.

Since it is well known, cf. for example [11, Chapter 1, Corollary 2.4], that condition (2.6) holds for $\varepsilon = 1$ it also holds for all $\varepsilon \in [0, 1]$ with the same constant α_0. Furthermore, condition (2.7) holds trivially with $\beta_0 = 1$ for $\varepsilon \in [0, 1]$.

3. Uniformly stable discretizations

The purpose of this section is to discuss finite element discretizations of the system (1.1). In particular, we shall be interested in discretizations which are stable uniformly in the parameter $\varepsilon \in (0, 1]$.

Let $\boldsymbol{V}_h \subset \boldsymbol{H}_0^1$ and $Q_h \subset L_0^2$ be finite element spaces, where $h \in (0, 1]$ is a discretization parameter. The weak formulation (2.4) leads to the following corresponding finite element discretization:

Find $(\boldsymbol{u}_h, p_h) \in \boldsymbol{V}_h \times Q_h$ such that

$$\begin{aligned} a_\varepsilon(\boldsymbol{u}_h, \boldsymbol{v}) + (p_h, \mathrm{div}\, \boldsymbol{v}) &= (\boldsymbol{f}, \boldsymbol{v}) \qquad \forall \boldsymbol{v} \in \boldsymbol{V}_h \\ (\mathrm{div}\, \boldsymbol{u}_h, q) &= (g, q) \qquad \forall q \in Q_h. \end{aligned} \tag{3.1}$$

Remark. Below we shall also encounter several examples of nonconforming approximations of (2.4), i.e. the space $\boldsymbol{V}_h \not\subseteq \boldsymbol{H}_0^1$. In all these examples the bilinear form $a_\varepsilon(\cdot, \cdot)$ is understood to be the sum of the corresponding integrals over each element. No extra jump terms are added. The same remark applies to the energy norm, $|\!|\!| \cdot |\!|\!|_\varepsilon$. □

The discretization (3.1) is stable in the sense of [6] if proper discrete analogs of the conditions (2.6) and (2.7) holds. These conditions are:

Stability conditions.
The discretization (3.1) is said to be uniformly stable if there exist constants $\alpha, \beta > 0$, independent of ε and h, such that

$$\sup_{\boldsymbol{v}\in \boldsymbol{V}_h} \frac{(q, \mathrm{div}\, \boldsymbol{v})}{|\!|\!| \boldsymbol{v} |\!|\!|_\varepsilon} \geq \alpha \|q\|_0 \quad \forall q \in Q_h, \tag{3.2}$$

and

$$a_\varepsilon(\boldsymbol{v}, \boldsymbol{v}) \geq \beta |\!|\!| \boldsymbol{v} |\!|\!|_\varepsilon^2 \quad \forall \boldsymbol{v} \in \boldsymbol{Z}_h, \tag{3.3}$$

where $\boldsymbol{Z}_h = \{\boldsymbol{v} \in \boldsymbol{V}_h : (\mathrm{div}\, \boldsymbol{v}, q) = 0 \quad \forall q \in Q_h\}$.

For the case $\varepsilon = 1$, or more precisely for ε bounded away from zero, the second condition is obvious. In this case there are several choices of pairs of finite element spaces which satisfies (3.2) with α independent

of h. We mention for example the Mini element proposed in [1] or the $P_2 - P_0$ element, i.e. we choose continuous quadratic velocities for $\boldsymbol{V}_h$ and the corresponding space of piecewise constants for Q_h, cf. [10]. For a general review of stable Stokes elements we refer to [8].

However, most of these spaces do *not* lead to discretizations which are stable uniformly in ε. The main reason for this is that when ε approaches zero the second condition is no longer obvious. In fact, for the reduced problem with $\varepsilon = 0$ the condition (3.3) requires

$$\|\boldsymbol{v}\|_0^2 \geq \beta \|\boldsymbol{v}\|_{\mathrm{div}}^2 \quad \forall \boldsymbol{v} \in \boldsymbol{Z}_h.$$

Hence, we must have

$$\|\operatorname{div} \boldsymbol{v}\|_0 \leq c\|\boldsymbol{v}\|_0 \quad \forall \boldsymbol{v} \in \boldsymbol{Z}_h \tag{3.4}$$

for a suitable constant c independent of h, and this condition does not hold for the common conforming stable Stokes elements.

Example 3.1 We consider the problem (1.1) with Ω taken as the unit square. The domain is triangulated by first dividing it into $h \times h$ squares. Then, each square is divided into two triangles by the diagonal with a negative slope. The system is then discretized using the $P_2 - P_0$ element with respect to this triangulation, i.e. $\boldsymbol{V}_h \subset \boldsymbol{H}_0^1$ consists of piecewise quadratic functions, while $Q_h \subset L_0^2$ is the space of discontinuous piecewise constants. This discretization is known to be stable when $\varepsilon > 0$ is fixed, cf. [10]. However, our purpose here is to investigate how the convergence behave as ε becomes small.

We consider the system (1.1) with the function g chosen to be identical zero, while $\boldsymbol{f} = \boldsymbol{u} - \varepsilon^2 \boldsymbol{\Delta u} - \mathbf{grad}\, p$, where $\boldsymbol{u} = \mathbf{curl} \sin^2(\pi x_1) \sin^2(\pi x_2)$ and $p = \sin(\pi x_1)$. Hence, in this example the solution is independent of ε.

In Table 3.1 below we have computed the relative L^2 error in the velocity $\boldsymbol{u}$, i.e. $e(h) = \|\boldsymbol{u} - \boldsymbol{u}_h\|_0 / \|\boldsymbol{u}\|_0$, for different values of ε and h. A third order Gauss-Legendre rule, cf. [17], was used here, and in all the other examples of this section, to perform the necessary integrations. For each fixed ε the convergence rate with respect to h, γ, is estimated by assuming $e(h) = ch^\gamma$, and by computing a least squares fit to this log–linear relation.

$\varepsilon \backslash$ h	2^{-2}	2^{-3}	2^{-4}	2^{-5}	2^{-6}	rate
1	3.84e-2	4.75e-3	6.41e-4	1.04e-4	2.11e-5	2.72
2^{-2}	6.15e-2	1.73e-2	4.65e-3	1.20e-3	3.05e-4	1.92
2^{-4}	4.55e-1	2.10e-1	6.78e-2	1.86e-2	4.79e-3	1.67
2^{-8}	9.31e-1	9.68e-1	9.43e-1	8.14e-1	5.32e-1	0.19
0	9.35e-1	9.84e-1	1.00	1.01	1.02	-0.03

TABLE 3.1. The relative L^2 error in velocity obtained by the $P_2 - P_0$ element.

When $\varepsilon = 1$ the convergence seems to be at least quadratic with respect to h in this case. However, the convergence deteriorates as ε becomes smaller, and for $\varepsilon = 0$ there is no convergence.

Table 3.2 is based on the corresponding relative errors in the energy norm, i.e. the norm $|||\cdot|||_\varepsilon$ for velocity and the L^2 norm for pressure. For simplicity only the estimated convergence rates are given.

ε	1	2^{-2}	2^{-4}	2^{-8}	0
rate, velocity	1.84	1.01	0.70	-0.79	-1.03
rate, pressure	1.06	1.01	1.09	0.13	-0.20

TABLE 3.2. Estimated convergence rates for the velocity and pressure, measured in the energy norm, for the $P_2 - P_0$ element.

These results indicate a similar degenerate behavior with respect to ε. In fact, when $\varepsilon = 0$ the norm, $|||\boldsymbol{u}_h|||_\varepsilon$, seems to grow like h^{-1} as h approach zero. This must be due to the fact that only the projection of $\operatorname{div} \boldsymbol{u}_h$ into piecewise constants is controlled by the method in this case. □

Example 3.2 We repeat the experiment above, but with the difference that we use the nonconforming Crouzeix–Raviart element instead of the $P_2 - P_0$ element, i.e. $\boldsymbol{V}_h$ consists of piecewise linear vector fields which are continuous at the midpoint of each edge of the triangulation, while $Q_h \subset L^2_0$ is the space of piecewise constants. It is well known that for any fixed $\varepsilon > 0$ this element leads to a stable discretization, cf. [10].

In Table 3.3 we have again computed the relative L^2 error in the velocity $\boldsymbol{u}$ for different values of ε and h.

$\varepsilon \backslash$ h	2^{-2}	2^{-3}	2^{-4}	2^{-5}	2^{-6}	rate
1	1.83e-1	4.89e-2	1.26e-2	3.19e-3	8.02e-4	1.96
2^{-2}	2.19e-1	6.89e-2	1.91e-2	4.96e-3	1.26e-3	1.87
2^{-4}	6.42e-1	3.86e-1	1.53e-1	4.58-2	1.21-3	1.45
2^{-8}	9.51e-1	1.00	1.01	9.43e-1	7.44e-1	0.08
0	9.53e-1	1.01	1.04	1.05	1.06	-0.04

TABLE 3.3. The relative L^2 error in velocity obtained by the nonconforming Crouzeix–Raviart element.

The L^2 convergence appears to be quadratic when ε is large. However, also in this case the convergence deteriorates as ε decreases, and for the reduced problem, with $\varepsilon = 0$, the observed values for the relative error is monotonically increasing.

The corresponding estimates of the the convergence rates in energy norm decreases from approximately linear convergence to no convergence as is shown by Table 3.4.

ε	1	2^{-2}	2^{-4}	2^{-8}	0
rate, velocity	0.98	0.97	0.74	0.03	-0.03
rate, pressure	1.00	0.93	0.98	0.12	-0.03

TABLE 3.4. Estimated convergence rates for the velocity and pressure, measured in the energy norm, for the Crouzeix–Raviart element.

In fact, the divergence of the Crouzeix–Raviart element in the case $\varepsilon = 0$ is not surprising. Since the divergence free vector fields in this case can be realized as the curl operator applied to the corresponding Morley space, this behavior of the Crouzeix–Raviart element is closely tied to the divergence of the Morley element for the Poisson equation, cf. [14]. □

The two examples above show that the $P_2 - P_0$ element and the nonconforming Crouzeix–Raviart element, which both are known to be stable for $\varepsilon = 1$, fail to give methods which converge uniformly in ε. The divergence of the $P_2 - P_0$ element for $\varepsilon = 0$ is basically due to the fact that the estimate (3.4) does not hold, and therefore the method is unstable, while the divergence of the Crouzeix–Raviart method is caused by the inconsistency of the method.

Example 3.3 We repeat the experiment above once more, but this time the system (1.1) is discretized by using the Mini element, i.e. $\boldsymbol{V}_h \subset \boldsymbol{H}_0^1$ consists of linear combinations of piecewise linear functions and cubic bubble functions with support on a single triangle, while $Q_h \subset L_0^2$ is the space of continuous piecewise linear functions.

In Table 3.5 below we have computed the relative error in the velocity, with respect to the energy norm $|||\cdot|||_\varepsilon$, for different values of ε and h.

$\varepsilon \backslash$ h	2^{-2}	2^{-3}	2^{-4}	2^{-5}	2^{-6}	rate
1	3.01	1.65	8.42e-1	4.22e-1	2.11e-1	0.96
2^{-2}	2.70	1.55	7.80e-1	3.90e-1	1.95e-1	0.96
2^{-4}	3.71	1.67	7.89e-1	3.87e-1	1.92e-1	1.07
2^{-8}	7.32	4.28	2.79	1.64	6.51e-1	0.84
0	7.44	4.76	3.70	3.39	3.30	0.28

TABLE 3.5. The relative error in velocity, measured in the energy norm, for the Mini element.

When $\varepsilon = 1$ the convergence seems to be linear with respect to h. This agrees with the theoretical results given in [1]. The convergence

deteriorates as ε becomes smaller, and for $\varepsilon = 0$ there seems to be essentially no convergence in the energy norm.

An interesting observation can be made for the Mini element if we consider the corresponding errors for the pressure p. In Table 3.6 below we study the relative error given by $\|p - p_h\|_0/\|p\|_0$.

$\varepsilon \backslash h$	2^{-2}	2^{-3}	2^{-4}	2^{-5}	2^{-6}	rate
1	8.78	2.81	8.85e-1	2.95e-1	1.02e-1	1.61
2^{-2}	6.09e-1	1.84e-1	5.62e-2	1.85e-2	6.40e-3	1.64
2^{-4}	6.08e-2	1.51e-2	3.88e-3	1.21e-3	4.07e-4	1.81
2^{-8}	3.58e-2	9.93e-3	2.34e-3	4.10e-4	6.00e-5	2.30
0	3.59e-2	1.02e-2	2.75e-3	7.23e-4	1.87e-4	1.90

TABLE 3.6. The relative L^2 error in the pressure obtained by the Mini element.

The surprising observation is that for the pressure the convergence seems to be uniform with respect to ε. In fact, the convergence rate seems to improve as ε tends to zero and for ε small the convergence with respect to h appears to be quadratic. This is a striking difference to what we observed in Examples 3.1 and 3.2. In both these cases the error in the pressure diverges as ε tend to zero, cf. Tables 3.2 and 3.4.

What we have observed here is not special to the present example. The Mini element leads to a discretization which is uniformly stable with respect to ε in a proper ε–dependent norm different from $|\!|\!| \cdot |\!|\!|_\varepsilon$. If we define the solution space $\boldsymbol{X}_\varepsilon$ by

$$\boldsymbol{X}_\varepsilon = (\boldsymbol{L}^2 \cap \varepsilon \cdot \boldsymbol{H}_0^1) \times ((\boldsymbol{H}^1 \cap L_0^2) + \varepsilon^{-1} \cdot L^2), \tag{3.5}$$

then it can be shown that the Mini element will in fact produce a uniformly stable discretization in the corresponding energy norm. This norm degenerates to the norm of $\boldsymbol{L}^2 \times H^1$ as ε tends to zero, cf. the discussion in Section 2 above. In order to confirm this behavior we computed the relative error in velocity once more, but this time we used the L^2 norm instead of $|\!|\!| \cdot |\!|\!|_\varepsilon$. The results are given in Table 3.7.

$\epsilon \backslash h$	2^{-2}	2^{-3}	2^{-4}	2^{-5}	2^{-6}	rate
1	3.54e-1	1.03e-1	2.64e-2	6.60e-3	1.65e-3	1.95
2^{-2}	3.16e-1	8.79e-2	2.20e-2	5.48e-3	1.37e-3	1.97
2^{-4}	1.90e-1	4.60e-2	1.07e-2	2.59e-3	6.42e-4	2.06
2^{-8}	1.81e-1	7.23e-2	2.87e-2	8.70e-3	1.74e-3	1.64
0	1.82e-1	7.66e-2	3.59e-2	1.76e-2	8.75e-3	1.09

TABLE 3.7. The relative L^2 error in velocity obtained by the Mini element.

We observe that as ε decreases from one to zero the corresponding convergence rate decreases from approximately two to one. However, there is no sign which indicates that the behavior will deteriorate below linear convergence. To complete the picture we have also computed the estimated convergence rates for the pressure in H^1. The results are given in Table 3.8.

ε	1	2^{-2}	2^{-4}	2^{-8}	0
rate	0.61	0.64	0.86	0.99	0.99

TABLE 3.8. Estimated convergence rates for the H^1 error of the pressure obtained by the Mini element.

The estimated convergence rate is clearly below one when $\varepsilon = 1$, while it improves towards one as ε is decreased. This is consistent with the fact that the norm of the pressure component of the product space (3.5) is weaker than the H^1 norm for each $\varepsilon > 0$, but approaches the H^1 norm as ε apprach zero.

The results above seem to confirm that the Mini element leads to a uniformly convergent discretization as long as the error is properly measured. However, as motivated in Section 2 above, in the present paper we are interested in a discretization of the system (1.1) which has a uniform behavior when the error is measured in $(\boldsymbol{H}_0(\mathrm{div}) \cap \varepsilon \cdot \boldsymbol{H}_0^1) \times L_0^2$. Therefore, for our purpose here, the Mini element should not be regarded as a uniformly stable element. □

Let us recall that if a standard conforming Stokes element is not uniformly stable with respect to ε, then this instability must be caused by the failure of the second stability condition (3.3), or equivalently (3.4). Note that the stability condition (3.4) will be trivially satisfied if the spaces $\boldsymbol{V}_h \times Q_h$ are constructed such that all elements of $\boldsymbol{Z}_h$ are divergence free, i.e. $\boldsymbol{Z}_h \subset \boldsymbol{Z}$. In fact, nearly all proposed finite element methods for the reduced problem will have this property. This is for example true for the Raviart–Thomas spaces, cf. [15], and for the Brezzi–Douglas–Marini spaces of [7]. However, in all these cases the spaces $\boldsymbol{V}_h$ will only be a subspace of $\boldsymbol{H}_0(\mathrm{div})$ and not of $\boldsymbol{H}_0^1$, due to the fact that only the normal components of the elements of $\boldsymbol{V}_h$ are required to be continuous across element edges. It is therefore not clear that these spaces will be useful for problems of the form (1.1) with $\varepsilon > 0$.

Example 3.4 We repeat the calculation done in the three examples above, but now we use the lowest order Raviart–Thomas space for the discretization. Hence, for $\varepsilon = 0$ we will expect to obtain linear convergence with respect to h. On the other hand, for $\varepsilon > 0$ the method is nonconforming and there seems to be no reason to expect that the method is convergent in this case. In Table 3.9 we have computed the

estimated convergence rates with respect to h for the relative L^2 errors of the velocity $\boldsymbol{u}$ and the pressure p for different values of ε.

ε	1	2^{-2}	2^{-4}	2^{-8}	0
rate, velocity	-0.07	-0.07	0.28	0.97	0.97
rate, pressure	-0.04	0.08	0.86	1.01	1.01

TABLE 3.9. Estimated convergence rates for the L^2 errors of the velocity and pressure for the Raviart–Thomas element.

As expected, the method appears to be divergent for $\varepsilon > 0$. □

4. A robust nonconforming finite element space

The four examples presented above illustrate that none of the standard elements, proposed for the case $\varepsilon = 1$ or $\varepsilon = 0$, will lead to a discrization of the problem (1.1) with uniform convergence properties with respect to ε, when the error is measured in the norm of the space $(\boldsymbol{H}_0(\mathrm{div}) \cap \varepsilon \cdot \boldsymbol{H}_0^1) \times L_0^2$. The purpose of the rest of this paper is therefore to construct and analyze a new finite element space which has this property.

4.1. **The finite element space.** In order to describe the new finite element space we will first define the proper polynomial space, or shape functions, on a given triangle. Let $T \subset \mathbb{R}^2$ be a triangle and consider the polynomial space of vector fields on T given by

$$\boldsymbol{V}(T) = \{\boldsymbol{v} \in \mathbb{P}_3^2 : \mathrm{div}\, \boldsymbol{v} \in \mathbb{P}_0, \quad (\boldsymbol{v} \cdot \boldsymbol{n})|_e \in \mathbb{P}_1 \quad \forall e \in \mathcal{E}(T)\}.$$

Here $\mathbb{P}_k$ denotes the set of polynomials of degree k and $\mathcal{E}(T)$ denotes the set of the edges of T. Furthermore, $\boldsymbol{n}$ is the unit normal vector on the edge e. Below we will also use $\boldsymbol{t}$ to denote the unit tangent vector on e, while τ denotes the arc length along e.

The space $\mathbb{P}_3^2$ is a vector space of dimension twenty. Furthermore, the conditions

$$\mathrm{div}\, \boldsymbol{v} \in \mathbb{P}_0 \quad \text{and} \quad (\boldsymbol{v} \cdot \boldsymbol{n})|_e \in \mathbb{P}_1 \quad \forall e \in \mathcal{E}(T),$$

represent at most eleven linearly independent constraints on this space. Therefore we must have

$$\dim \boldsymbol{V}(T) \geq 9.$$

In fact, we shall show that $\dim \boldsymbol{V}(T) = 9$.

Lemma 4.1. *The space $\boldsymbol{V}(T)$ is a linear space of dimension nine. Furthermore, an element $\boldsymbol{v} \in \boldsymbol{V}(T)$ is uniquely determined by the following degrees of freedom:*

- $\int_e (\boldsymbol{v} \cdot \boldsymbol{n}) \tau^k \, d\tau \quad k = 0, 1 \quad$ *for all* $e \in \mathcal{E}(T)$.
- $\int_e (\boldsymbol{v} \cdot \boldsymbol{t}) \, d\tau \quad$ *for all* $e \in \mathcal{E}(T)$.

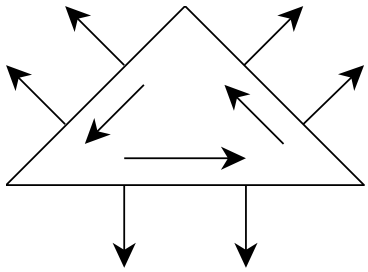

FIGURE 4.1. The degrees of freedom of the new nonconforming element.

Proof. Since $\boldsymbol{V}(T)$ is a vector space of dimension ≥ 9 it is enough to show that elements of $\boldsymbol{V}(T)$ are uniquely determined by the given nine degrees of freedom. Assume that $\boldsymbol{v} \in \boldsymbol{V}(T)$ with all the degrees of freedom equal zero. In particular, this implies that

$$(\boldsymbol{v} \cdot \boldsymbol{n})|_{\partial T} \equiv 0.$$

As a consequence of this

$$\int_T \operatorname{div} \boldsymbol{v}\, dx = \int_{\partial T} \boldsymbol{v} \cdot \boldsymbol{n}\, d\tau = 0.$$

Hence, since $\operatorname{div} \boldsymbol{v} \in \mathbb{P}_0$, we conclude that $\boldsymbol{v}$ is divergence free.

However, since $\boldsymbol{v} \in \mathbb{P}_3^2$ is divergence free we must have $\boldsymbol{v} = \mathbf{curl}\, w$ for a suitable scalar function $w \in \mathbb{P}_4$. Furthermore, since

$$(\mathbf{grad}\, w \cdot \boldsymbol{t})|_e = (\boldsymbol{v} \cdot \boldsymbol{n})|_e = 0$$

for each edge e, we conclude that $\mathbf{grad}\, w \cdot \boldsymbol{t} \equiv 0$ on ∂T. Since w is uniquely determined only up to a constant, we can therefore assume that $w \equiv 0$ on ∂T.

Hence, w is of the form $w = pb$, where $p \in \mathbb{P}_1$ and b is the cubic bubble function with respect to T, i.e. $b = \lambda_1\lambda_2\lambda_3$, where $\lambda_i(x)$ are the barycentric coordinates of x with respect to the three corners of T. In particular, $\frac{\partial b}{\partial \boldsymbol{n}}|_e$ does not change sign on e. Furthermore,

$$\frac{\partial w}{\partial \boldsymbol{n}}|_{\partial T} = p\frac{\partial b}{\partial \boldsymbol{n}}|_{\partial T},$$

and

$$\int_e p\frac{\partial b}{\partial \boldsymbol{n}}\, d\tau = \int_e \frac{\partial w}{\partial \boldsymbol{n}}\, d\tau = \int_e \boldsymbol{v} \cdot \boldsymbol{t}\, d\tau = 0 \quad \forall e \in \mathcal{E}(T).$$

We can therefore conclude that p has a root in the interior of e. However, if $p \in \mathbb{P}_1$ with a root in the interior of each edge of T then $p \equiv w \equiv 0$. □

Let $\{\mathcal{T}_h\}$ be a shape regular family of triangulations of Ω, where h is the maximal diameter. Furthermore, let $\mathcal{E}_h$ be the set of edges of $\mathcal{T}_h$.

Define a finite element space of vector fields $\boldsymbol{V}_h$, associated with the triangulation $\mathcal{T}_h$, as all functions $\boldsymbol{v} \in \boldsymbol{V}_h$ such that

- $\boldsymbol{v}|_T \in \boldsymbol{V}(T)$ for all $T \in \mathcal{T}_h$
- $\int_e (\boldsymbol{v} \cdot \boldsymbol{n}) \tau^k \, d\tau$ is continuous for $k = 0, 1$ for all $e \in \mathcal{E}_h$,
- $\int_e (\boldsymbol{v} \cdot \boldsymbol{t}) \, d\tau$ is continuous for all $e \in \mathcal{E}_h$.

Here we assume that $\boldsymbol{v}$ is extended to be zero outside Ω, i.e. if e is an edge on the boundary of Ω then we require

$$\int_e (\boldsymbol{v} \cdot \boldsymbol{n}) \tau^k \, d\tau = 0 \qquad k = 0, 1 \quad \text{and} \quad \int_e (\boldsymbol{v} \cdot \boldsymbol{t}) \, d\tau = 0.$$

It follows from Lemma 4.1 that any function $\boldsymbol{v} \in \boldsymbol{V}_h$ is uniquely determined by the two lowest order moments of $\boldsymbol{v} \cdot \boldsymbol{n}$ and by the mean value of $\boldsymbol{v} \cdot \boldsymbol{t}$ for all interior edges, cf. Figure 4.1.

If $\boldsymbol{v} \in \boldsymbol{V}_h$ then the normal component $\boldsymbol{v} \cdot \boldsymbol{n}$ is continuous for all interior edges. Therefore, $\boldsymbol{V}_h \subset \boldsymbol{H}_0(\mathrm{div})$. However, the tangential component of $\boldsymbol{v}$ is not continuous, only the mean value with respect to each edge is continuous. Therefore, $\boldsymbol{V}_h \not\subseteq \boldsymbol{H}_0^1$. In addition to the space $\boldsymbol{V}_h$ we let $Q_h \subset L_0^2$ denote the space of scalar piecewise constants with respect to the triangulation $\mathcal{T}_h$.

In the rest of this paper $\boldsymbol{V}_h$ and Q_h will always refer to the finite element spaces just introduced. The corresponding nonconforming finite element approximation of the system (1.1) is defined by the system (3.1).

4.2. **Properties of the new finite element space.** It follows from the definition of $\boldsymbol{V}_h$ that $\operatorname{div} \boldsymbol{V}_h \subset Q_h$. Hence, if we define $\boldsymbol{Z}_h \subset \boldsymbol{V}_h$ as the weakly divergence free elements of $\boldsymbol{V}_h$, i.e.

$$\boldsymbol{Z}_h = \{\boldsymbol{v} \in \boldsymbol{V}_h : (\operatorname{div} \boldsymbol{v}, q) = 0 \quad \forall q \in Q_h\},$$

then these elements are in fact divergence free.

Remark. It can be seen that

$$\boldsymbol{Z}_h = \mathbf{curl}\, W_h, \tag{4.1}$$

where W_h is an associated nonconforming H^2–element. Locally, on each triangle, W_h consists of all $\mathbb{P}_4$ polynomials which reduces to a quadratic on each edge. In addition, $W_h \subset H_0^1$ and the average of the normal derivatives of functions in W_h are continuous on on each edge. The finite element space W_h is precisely described and analyzed in [14]. The identity (4.1) was actually the main motivation for the construction of the space $\boldsymbol{V}_h$. More precisely, the spaces W_h, $\boldsymbol{V}_h$ and Q_h are related such that the sequence

$$0 \longrightarrow W_h/\mathbb{R} \xrightarrow{\mathbf{curl}} \boldsymbol{V}_h \xrightarrow{\operatorname{div}} Q_h \longrightarrow 0.$$

is exact. In particular, $\operatorname{div} \boldsymbol{V}_h = Q_h$. $\square$

Define an interpolation operator $\boldsymbol{\Pi}_h : \boldsymbol{H}_0^1 \mapsto \boldsymbol{V}_h$ by

$$\int_e (\boldsymbol{\Pi}_h \boldsymbol{v} \cdot \boldsymbol{n}) \tau^k \, d\tau = \int_e (\boldsymbol{v} \cdot \boldsymbol{n}) \tau^k \, d\tau \quad k = 0, 1$$
$$\int_e (\boldsymbol{\Pi}_h \boldsymbol{v} \cdot \boldsymbol{t}) \, d\tau = \int_e (\boldsymbol{v} \cdot \boldsymbol{t}) \, d\tau$$

for all $e \in \mathcal{E}_h$. In addition, let $P_h : L_0^2 \mapsto Q_h$ be the L^2–projection. From the definition of the operator $\boldsymbol{\Pi}_h$ we easily verify the commutativity property

$$\operatorname{div} \boldsymbol{\Pi}_h \boldsymbol{v} = P_h \operatorname{div} \boldsymbol{v} \quad \text{for all } \boldsymbol{v} \in \boldsymbol{H}_0^1. \tag{4.2}$$

In fact, for all $T \in \mathcal{T}_h$

$$\int_T \operatorname{div} \boldsymbol{\Pi}_h \boldsymbol{v} \, dx = \int_{\partial T} (\boldsymbol{\Pi}_h \boldsymbol{v} \cdot \boldsymbol{n}) \, d\tau = \int_{\partial T} (\boldsymbol{v} \cdot \boldsymbol{n}) \, d\tau = \int_T \operatorname{div} \boldsymbol{v} \, dx$$

and hence (4.2) follows.

Since Q_h is the space of piecewise constants the L^2–projection P_h onto Q_h satisfies

$$\|w - P_h w\|_0 \le ch \|w\|_1 \tag{4.3}$$

for all $w \in H^1 \cap L_0^2$, where $c > 0$ is independent of h and w. The operator $\boldsymbol{\Pi}_h$ is well defined on $\boldsymbol{H}_0^1$, it is locally defined on each triangle, and it preserves linear functions locally. Furthermore, the polynomial space $\boldsymbol{V}(T)$ is invariant under affine Piola transformations. More precisely, let $T \in \mathcal{T}_h$ and $\phi(x) = Bx + c$ an affine map of T onto a reference triangle $\hat{T}$. Then the Piola transform, $\boldsymbol{v} \mapsto \hat{\boldsymbol{v}}$, where

$$\hat{\boldsymbol{v}}(\hat{x}) = (\det B)^{-1} B v(x), \qquad \hat{x} = \phi(x),$$

maps $\boldsymbol{V}(T)$ onto $\boldsymbol{V}(\hat{T})$. Therefore, approximation estimates for the operator $\boldsymbol{\Pi}_h$ can be derived from standard scaling arguments utilizing the shape regularity of $\{\mathcal{T}_h\}$. In particular, there exists a constant $c > 0$, independent of h such that

$$\|\boldsymbol{\Pi}_h \boldsymbol{v}\|_{\operatorname{div}} \le \|\boldsymbol{\Pi}_h \boldsymbol{v}\|_{1,h} \le c \|\boldsymbol{v}\|_1. \tag{4.4}$$

In addition, from the Bramble–Hilbert lemma, using the fact that $\boldsymbol{\Pi}_h$ preserves linears locally, we can further conclude that

$$\|\boldsymbol{\Pi}_h \boldsymbol{v} - \boldsymbol{v}\|_{j,h} \le ch^{k-j} |\boldsymbol{v}|_k \qquad \text{for } 0 \le j \le 1 \le k \le 2, \tag{4.5}$$

and for all $\boldsymbol{v} \in \boldsymbol{H}_0^1 \cap \boldsymbol{H}^k$. Here $\|\cdot\|_{j,h}$ denotes the piecewise $\boldsymbol{H}^j$–norm

$$\|\boldsymbol{v}\|_{j,h}^2 = \sum_{T \in \mathcal{T}_h} \|\boldsymbol{v}\|_{j,T}^2.$$

In fact, if $\hat{T}$ is a reference triangle, and $\hat{\boldsymbol{\Pi}} : \boldsymbol{H}^1(\hat{T}) \mapsto \boldsymbol{V}(\hat{T})$ the corresponding interpolation operator, then for all $\boldsymbol{v} \in H^1(\hat{T})$

$$\|\hat{\boldsymbol{\Pi}} \boldsymbol{v}\|_{0,\hat{T}} \le c_1 \|\boldsymbol{v}\|_{0,\partial\hat{T}} \le c_2 \|\boldsymbol{v}\|_{0,\hat{T}}^{1/2} \|\boldsymbol{v}\|_{1,\hat{T}}^{1/2},$$

where c_1 and c_2 only depends on $\hat{T}$. Hence, from a scaling argument we also obtain the low order estimate

$$\|\boldsymbol{\Pi}_h \boldsymbol{v} - \boldsymbol{v}\|_0 \leq c h^{1/2} \|\boldsymbol{v}\|_0^{1/2} \|\boldsymbol{v}\|_1^{1/2} \tag{4.6}$$

for all $\boldsymbol{v} \in \boldsymbol{H}_0^1$.

Next we will verify the stability conditions (3.2) and (3.3) for the product space $\boldsymbol{V}_h \times Q_h$. However, due to the fact that we are considering a nonconforming finite element approximation of the system (1.1), where $\boldsymbol{V}_h \not\subseteq \boldsymbol{H}_0^1$, the norm $|\!|\!| \cdot |\!|\!|_\varepsilon$ has to be properly modified. For each $\boldsymbol{v} \in \boldsymbol{V}_h$ we define

$$|\!|\!| \boldsymbol{v} |\!|\!|_{\varepsilon,h}^2 = \|\boldsymbol{v}\|_{\mathrm{div}}^2 + \varepsilon^2 \sum_{T \in \mathcal{T}_h} \|\boldsymbol{D}\boldsymbol{v}\|_{0,T}^2.$$

Note that for $\varepsilon = 0$ this norm is simply equal to $\|\cdot\|_{\mathrm{div}}$, while for $\varepsilon = 1$ it is equivalent, uniformly in h, to the piecewise $\boldsymbol{H}^1$–norm $\|\cdot\|_{1,h}$.

Lemma 4.2. *There exists a constant $\alpha_1 > 0$, independent of h, such that*

$$\sup_{\boldsymbol{v} \in \boldsymbol{V}_h} \frac{(q, \operatorname{div} \boldsymbol{v})}{\|\boldsymbol{v}\|_{1,h}} \geq \alpha_1 \|q\|_0 \quad \textit{for all } q \in Q_h.$$

Proof. This follows by a standard argument from the properties of the interpolation operator $\boldsymbol{\Pi}_h$ and the corresponding continuous result (2.6). In fact, since for any $\boldsymbol{v} \in \boldsymbol{H}_0^1$ and $q \in Q_h$ we have

$$(q, \operatorname{div} \boldsymbol{\Pi}_h \boldsymbol{v}) = (q, \operatorname{div} \boldsymbol{v})$$

and

$$\|\boldsymbol{\Pi}_h \boldsymbol{v}\|_{1,h} \leq c_1 \|\boldsymbol{v}\|_1,$$

we can take $\alpha_1 = \alpha_0 / c_1$. □

The following uniform stability result is an immediate consequence of the previous lemma.

Theorem 4.1. *The pair of spaces $(\boldsymbol{V}_h, Q_h)$ satisfies the uniform stability conditions* (3.2) *and* (3.3)*, but with the norm $|\!|\!| \cdot |\!|\!|_\varepsilon$ replaced by $|\!|\!| \cdot |\!|\!|_{\varepsilon,h}$.*

Proof. The norms $|\!|\!| \cdot |\!|\!|_{1,h}$ and $\|\cdot\|_{1,h}$ are equivalent on $\boldsymbol{V}_h$ and $|\!|\!| \cdot |\!|\!|_{\varepsilon,h}$ decreases as ε decreases. It follows from Lemma 4.2 that condition (3.2) holds. Since $\boldsymbol{Z}_h \subset \boldsymbol{Z}$ the second condition (3.3) holds with $\beta = 1$. □

5. Error estimates for smooth solutions

Since our new finite element space $(\boldsymbol{V}_h, Q_h)$ satisfies the proper stability conditions (3.2) and (3.3), uniformly with respect to ε, it seems probable that the corresponding finite element method will in fact have uniform convergence properties. In the present section we shall investigate this question under the assumption that the solution (u, p) of the continuous problem is sufficiently smooth, while the effect of the

ε–dependent boundary layers will be taken into account in the next section.

We will start the discussion here with a numerical example which is completely similar to Examples 3.1–3.3.

Example 5.1 We redo the computations done in Examples 3.1–3.3, but this time we use the finite element spaces constructed above. In all the numerical examples with the the new element we used a fifth order Gauss-Legendre method, cf. [17], as integration rule.

In Table 5.1 we have computed the estimated convergence rates with respect to h for the velocity and the pressure.

ε	1	2^{-2}	2^{-4}	2^{-8}	0
rate, velocity in L^2	1.93	1.94	1.94	1.90	1.92
rate, velocity in $\|\!\|\!\| \cdot \|\!\|\!\|_\varepsilon$	0.98	0.99	1.05	1.72	1.92
rate, pressure in L^2	0.98	1.00	1.00	1.00	1.00

TABLE 5.1. Estimated convergence rates for the velocity and the pressure for the new nonconforming element.

We observe that the convergence rates in L^2 appear to be close to quadratic in velocity and linear in pressure uniformly with respect to $\varepsilon \in [0, 1]$, while the convergence in the energy norm appears to be at least linear for each $\varepsilon > 0$. In fact, as ε approaches zero the convergence rate tends to two. This improved convergence is partly due to the fact that the exact solution $\boldsymbol{u}$ is divergence free in this case.

To make a direct comparison between the $P_2 - P_0$ element, the Crouzeix–Raviart element, the Mini element, and the new element when ε is small compared to h, we have plotted the errors in velocity for the different methods as functions of σ, where $h = 2^{-\sigma}$. Here we have chosen $\varepsilon = 2^{-8}$. The errors are plotted, in a logarithmic scale, in Figure 5.1.

To the left the L^2 errors are plotted, while the errors in the energy norm are depicted to the right. We observe that the Mini element and the new element bahaves comparably with respect to the L^2 norm, while the new element clearly is superior to all the other methods with respect to the energy norm. □

The rest of this section will be devoted to establishing error estimates for the new nonconforming finite element method. Throughout this section we will assume that $\boldsymbol{u} \in \boldsymbol{H}^2 \cap \boldsymbol{H}_0^1$, where $(\boldsymbol{u}, p)$ is the weak solution of (2.4). For convenience we also introduce the notation $\|\cdot\|_a$ for the norm on $\boldsymbol{V}_h$ associated the bilinear form a_ε, i.e.

$$\|\boldsymbol{v}\|_a^2 = \|\boldsymbol{v}\|_0^2 + \sum_{T \in \mathcal{T}_h} \|\boldsymbol{D}\boldsymbol{v}\|_{0,T}^2.$$

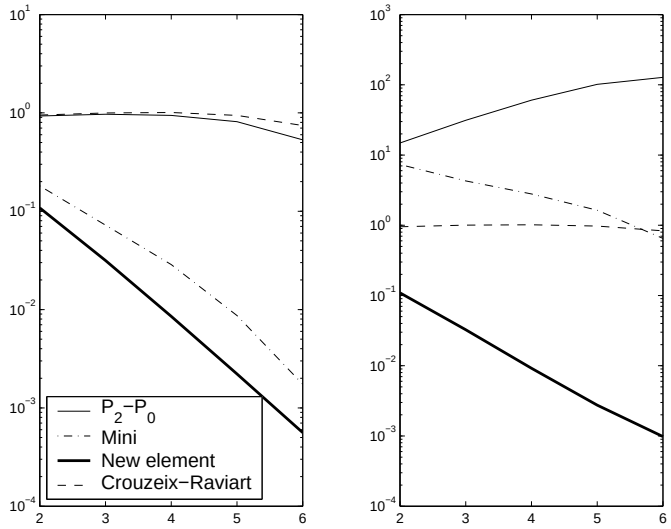

FIGURE 5.1. The errors in velocity, measured in the L^2 norm and the energy norm, as functions of $\sigma = -\log(h)/\log(2)$.

For any $\boldsymbol{v} \in \boldsymbol{V}_h$, we define the consistency error $E_{\varepsilon,h}(\boldsymbol{u}, \boldsymbol{v})$ by

$$E_{\varepsilon,h}(\boldsymbol{u}, \boldsymbol{v}) = \varepsilon^2 \sum_{e \in \mathcal{E}_h} \int_e (\operatorname{rot} \boldsymbol{u}) \ [\boldsymbol{v} \cdot \boldsymbol{t}] \, d\tau.$$

Here, if T_- and T_+ are two triangles, sharing an edge e, then $[w] = [w]_e = w|_{T_+} - w|_{T_-}$ denotes the jump of w across e, while $\boldsymbol{t}$ is the unit tangent vector along e corresponding to the clockwise direction on T_+. Since $[\boldsymbol{v} \cdot \boldsymbol{n}]_e = 0$ for any $\boldsymbol{v} \in \boldsymbol{V}_h$ it follows from (2.2) and Green's theorem, in particular from (2.1), that

$$\begin{aligned} a_\varepsilon(\boldsymbol{u}, \boldsymbol{v}) + (p, \operatorname{div} \boldsymbol{v}) &= (\boldsymbol{f}, \boldsymbol{v}) + E_{\varepsilon,h}(\boldsymbol{u}, \boldsymbol{v}) && \forall \boldsymbol{v} \in \boldsymbol{V}_h, \\ (\operatorname{div} \boldsymbol{u}, q) &= (g, q) && \forall q \in L^2_0, \end{aligned} \tag{5.1}$$

where the term $E_{\varepsilon,h}$ appears due to the fact that $\boldsymbol{V}_h \not\subseteq \boldsymbol{H}^1_0$.

In the error analysis below we will need proper estimates on the consistency error $E_{\varepsilon,h}$. The following bounds are therefore useful.

Lemma 5.1. *If $\boldsymbol{u} \in \boldsymbol{H}^2 \cap \boldsymbol{H}^1_0$ then*

$$\sup_{\boldsymbol{v} \in \boldsymbol{V}_h} \frac{|E_{\varepsilon,h}(\boldsymbol{u}, \boldsymbol{v})|}{\|\boldsymbol{v}\|_a} \le c\, \varepsilon \begin{cases} h \| \operatorname{rot} \boldsymbol{u}\|_1 \\ h^{1/2} \| \operatorname{rot} \boldsymbol{u}\|_1^{1/2} \| \operatorname{rot} \boldsymbol{u}\|_0^{1/2}, \end{cases}$$

where $c > 0$ is independent of ε and h.

Proof. Let $e \in \mathcal{E}_h$ and $\boldsymbol{v} \in \boldsymbol{H}^1_0 + \boldsymbol{V}_h$. Since the mean value with respect to e of $\boldsymbol{v} \cdot \boldsymbol{t}$ is zero, it follows from a standard scaling argument, cf. for example [5, Section 8.3] or [14, Section 4] for similar arguments, that

for any $\phi \in H^1$

$$\begin{aligned} \textstyle\int_e \phi[\boldsymbol{v}\cdot\boldsymbol{t}]d\tau &\le \inf_{\lambda,\mu\in\mathbb{R}} \|\phi-\lambda\|_{0,e}\|[\boldsymbol{v}\cdot\boldsymbol{t}-\mu]\|_{0,e} \\ &\le \begin{cases} ch|\phi|_{1,\Omega_e}(|\boldsymbol{v}|_{1,T_-}+|\boldsymbol{v}|_{1,T_+}) \\ ch^{1/2}|\phi|^{1/2}_{1,\Omega_e}\|\phi\|^{1/2}_{0,\Omega_e}(|\boldsymbol{v}|_{1,T_-}+|\boldsymbol{v}|_{1,T_+}). \end{cases} \end{aligned} \tag{5.2}$$

Here T_- and T_+ denote the two triangles meeting the edge e and $\Omega_e = T_-\cup T_+$. Since

$$|E_{\varepsilon,h}(\boldsymbol{u},\boldsymbol{v})| \le \varepsilon^2 \sum_{e\in\mathcal{E}_h} |\int_e (\operatorname{rot}\boldsymbol{u})\ [\boldsymbol{v}\cdot\boldsymbol{t}]\,d\tau|,$$

the desired estimate follows by applying the estimate (5.2) with $\phi = \operatorname{rot}\boldsymbol{u}$, summing over all edges, and using the fact that

$$\sum_{e\in\mathcal{E}_h} |\boldsymbol{v}|^2_{1,T} \le \varepsilon^{-2} a_\varepsilon(\boldsymbol{v},\boldsymbol{v}).$$

□

Let $(\boldsymbol{u}_h, p_h) \in \boldsymbol{V}_h \times Q_h$ be the approximation of $(\boldsymbol{u}, p)$ derived from the discrete system (3.1). From (3.1) and (5.1) we obtain

$$a_\varepsilon(\boldsymbol{u}-\boldsymbol{u}_h,\boldsymbol{v}) + (p-p_h, \operatorname{div}\boldsymbol{v}) = E_{\varepsilon,h}(\boldsymbol{u},\boldsymbol{v}) \tag{5.3}$$

for all $\boldsymbol{v}\in\boldsymbol{V}_h$. Furthermore,

$$\operatorname{div}\boldsymbol{u}_h = P_h \operatorname{div}\boldsymbol{u} = \operatorname{div}\boldsymbol{\Pi}_h\boldsymbol{u}.$$

Therefore, taking $\boldsymbol{v} = \boldsymbol{\Pi}_h\boldsymbol{u} - \boldsymbol{u}_h$ in (5.3) we obtain

$$a_\varepsilon(\boldsymbol{u}-\boldsymbol{u}_h, \boldsymbol{\Pi}_h\boldsymbol{u}-\boldsymbol{u}_h) = E_{\varepsilon,h}(\boldsymbol{u}, \boldsymbol{\Pi}_h\boldsymbol{u}-\boldsymbol{u}_h).$$

Since a_ε is an inner product we further have

$$\begin{aligned} \|\boldsymbol{\Pi}_h\boldsymbol{u}-\boldsymbol{u}_h\|_a^2 &\le \|\boldsymbol{u}-\boldsymbol{\Pi}_h\boldsymbol{u}\|_a^2 + 2a_\varepsilon(\boldsymbol{u}-\boldsymbol{u}_h, \boldsymbol{\Pi}_h\boldsymbol{u}-\boldsymbol{u}_h) \\ &\le \|\boldsymbol{u}-\boldsymbol{\Pi}_h\boldsymbol{u}\|_a^2 + 2E_{\varepsilon,h}(\boldsymbol{u}, \boldsymbol{\Pi}_h\boldsymbol{u}-\boldsymbol{u}_h). \end{aligned}$$

Hence, we conclude that

$$\|\boldsymbol{u}-\boldsymbol{u}_h\|_a \le 2(\|\boldsymbol{u}-\boldsymbol{\Pi}_h\boldsymbol{u}\|_a + \sup_{\boldsymbol{v}\in\boldsymbol{V}_h} \frac{|E_{\varepsilon,h}(\boldsymbol{u},\boldsymbol{v})|}{\|\boldsymbol{v}\|_a}). \tag{5.4}$$

From this basic bound we easily derive the following error estimate.

Theorem 5.1. *If $\boldsymbol{u}\in\boldsymbol{H}^2\cap\boldsymbol{H}^1_0$ and $p\in H^1\cap L^2_0$ then the following estimates hold:*

$$\begin{aligned} \|\boldsymbol{u}-\boldsymbol{u}_h\|_0 + \varepsilon\|\operatorname{rot}(\boldsymbol{u}-\boldsymbol{u}_h)\|_0 &\le c(h^2+\varepsilon h)\|\boldsymbol{u}\|_2, \\ \|\operatorname{div}(\boldsymbol{u}-\boldsymbol{u}_h)\|_0 &\le ch\|\operatorname{div}\boldsymbol{u}\|_1 \\ \|p-p_h\|_0 &\le ch(\|p\|_1 + (\varepsilon+h)\|\boldsymbol{u}\|_2). \end{aligned}$$

Here $c>0$ is a constant independent of ε and h.

Remark: Here, and below, the differential operators $\boldsymbol{D}$ and rot, applied to vector fiels in $\boldsymbol{V}_h$, are defined locally on each triangle of the triangulation $\mathcal{T}_h$. □

Proof. The first estimate is a direct consequence of (4.5), (5.4), and Lemma 5.1. The second estimate follows from the bound (4.3), and the fact that $\operatorname{div} \boldsymbol{u}_h = P_h \operatorname{div} \boldsymbol{u}$.

In order to establish the third estimate we first observe that (4.3) implies that

$$\|p - P_h p\|_0 \leq ch\|p\|_1. \tag{5.5}$$

Hence, it only remains to estimate $P_h p - p_h$. However, from the modified inf–sup condition (3.2), cf. Theorem 4.1, we obtain

$$\|P_h p - p_h\|_0 \leq \alpha^{-1} \sup_{\boldsymbol{v} \in \boldsymbol{V}_h} \frac{(P_h p - p_h, \operatorname{div} \boldsymbol{v})}{|\!|\!| \boldsymbol{v} |\!|\!|_{\varepsilon,h}}.$$

Furthermore, for any $\boldsymbol{v} \in \boldsymbol{V}_h$ we have

$$\begin{aligned}(P_h p - p_h, \operatorname{div} \boldsymbol{v}) &= (p - p_h, \operatorname{div} \boldsymbol{v}) \\ &= -a_\varepsilon(\boldsymbol{u} - \boldsymbol{u}_h, \boldsymbol{v}) + E_{\varepsilon,h}(\boldsymbol{u}, \boldsymbol{v}),\end{aligned}$$

which implies that

$$|(P_h p - p_h, \operatorname{div} \boldsymbol{v})| \leq (\|\boldsymbol{u} - \boldsymbol{u}_h\|_a + \sup_{\boldsymbol{v} \in \boldsymbol{V}_h} \frac{|E_{\varepsilon,h}(\boldsymbol{u}, \boldsymbol{v})|}{\|\boldsymbol{v}\|_a}) |\!|\!| \boldsymbol{v} |\!|\!|_{\varepsilon,h},$$

or

$$\|P_h p - p_h\|_0 \leq \alpha^{-1}(\|\boldsymbol{u} - \boldsymbol{u}_h\|_a + \sup_{\boldsymbol{v} \in \boldsymbol{V}_h} \frac{|E_{\varepsilon,h}(\boldsymbol{u}, \boldsymbol{v})|}{\|\boldsymbol{v}\|_a}). \tag{5.6}$$

From the previous estimates we therefore obtain

$$\|P_h p - p_h\|_0 \leq c(h^2 + \varepsilon h)\|\boldsymbol{u}\|_2,$$

and together with (5.5) this establishes the desired estimate on the error $\|p - p_h\|_0$. □

Remark: As an alternative to the estimates given in Theorem 5.1 above we can also obtain

$$\|\boldsymbol{u} - \boldsymbol{u}_h\|_0 + \varepsilon \|\operatorname{rot}(\boldsymbol{u} - \boldsymbol{u}_h)\|_0 \leq ch(\|\boldsymbol{u}\|_1 + \varepsilon\|\boldsymbol{u}\|_2) \tag{5.7}$$

and

$$\|p - p_h\|_0 \leq ch(\|p\|_1 + \|\boldsymbol{u}\|_1 + \varepsilon\|\boldsymbol{u}\|_2). \tag{5.8}$$

These modifications are obtained if we use the estimate

$$\|\boldsymbol{u} - \boldsymbol{\Pi}_h \boldsymbol{u}\|_0 \leq ch\|\boldsymbol{u}\|_1,$$

obtained from (4.5), in (5.4) instead of the corresponding quadratic estimate. Even if the modified estimates are weaker for uniformly smooth solutions, they are sometimes preferable for more singular solutions. □

6. Boundary layers and uniform error estimates

In general, we cannot expect that the norm $\|\boldsymbol{u}\|_2$ of the solution of (1.1) is bounded independently of ε. In fact, as ε approach zero even $\|\operatorname{rot}\boldsymbol{u}\|_0$ should be expected to blow up. Hence, the convergence estimates given in Theorem 5.1 will deteriorate as ε becomes small. The following example shows that this behavior of the error is in fact real.

Example 6.1 In this example we study the convergence for an ε dependent solution. Let $\boldsymbol{u} = \varepsilon\,\mathbf{curl}\, e^{-x_1x_2/\varepsilon}$, $p = \varepsilon e^{-x_1/\varepsilon}$, $\boldsymbol{f} = \boldsymbol{u} - \varepsilon^2\boldsymbol{\Delta u} - \mathbf{grad}\, p$ and g identical zero. In fact, $\boldsymbol{u}$ is not the solution of the corresponding system (1.1), since the boundary conditions are not satisfied. However, the adaption of the new method to nonhomogeneous boundary conditions is straightforward.

The significance of the solution $\boldsymbol{u}$ just given is related to the fact that the quantities $\|\operatorname{rot}\boldsymbol{u}\|_0$ and $\varepsilon\|\operatorname{rot}\boldsymbol{u}\|_1$ both are of order $\varepsilon^{-1/2}$ as ε tends to zero. As we will see below, in Lemma 6.1, this behavior is typical for solutions of the singular perturbation problem (1.1). For solutions with this singular behavior the estimates (5.7) and (5.8) leads to error bounds of the form

$$|||\boldsymbol{u} - \boldsymbol{u}_h|||_\varepsilon, \|p - p_h\|_0 \le ch\varepsilon^{-1/2}, \tag{6.1}$$

where c is a constant independent of ε and h. In Table 6.1 below we have computed the absolute error, $|||\boldsymbol{u} - \boldsymbol{u}_h|||_\varepsilon$ for different values of ε and h. For each fixed ε the convergence rate with respect to h is estimated.

$\varepsilon\backslash$ h	2^{-2}	2^{-3}	2^{-4}	2^{-5}	2^{-6}	rate
2^{-2}	7.29e-2	3.60e-2	1.77e-2	8.75e-3	4.36e-3	0.98
2^{-6}	8.89e-2	5.88e-2	3.71e-2	2.06e-2	1.05e-2	0.77
2^{-8}	1.12e-1	6.89e-2	4.07e-2	2.66e-2	1.73e-2	0.67
2^{-10}	1.17e-1	8.16e-2	5.48e-2	3.34e-2	1.93e-2	0.65
2^{-12}	1.17e-1	8.20e-2	5.74e-2	4.02e-2	2.71e-2	0.52

Table 6.1. The absolute error in velocity, measured in the energy norm, obtained by the new nonconforming element.

We observe that for ε sufficiently large the convergence rate is approximately one, but the estimated rate decreases when ε approaches zero. These results seem to confirm the claim that the convergence is linear with respect to h for each fixed ε. However, when h is sufficiently large compared to ε we do not observe this linear rate.

In Table 6.2 we give the corresponding absolute L^2 errors for the pressure.

$\varepsilon \backslash$ h	2^{-2}	2^{-3}	2^{-4}	2^{-5}	2^{-6}	rate
2^{-2}	2.32e-2	1.11e-2	5.36e-3	2.64e-3	1.31e-3	1.04
2^{-6}	9.00e-3	5.33e-3	2.62e-3	1.15e-3	4.61e-4	1.07
2^{-8}	5.28e-3	3.24e-3	2.18e-3	1.23e-3	5.97e-4	0.77
2^{-10}	4.93e-3	2.54e-3	1.33e-3	7.93e-4	5.32e-4	0.81
2^{-12}	4.92e-3	2.51e-3	1.24e-3	6.22e-4	3.27e-4	0.98

TABLE 6.2. The absolute L^2 error in the pressure obtained by the new nonconforming element.

Again the estimated convergence rate is approximately one for ε large. Then it starts to decrease with ε as in Table 6.1. However, in this case the convergence rate increases roughly back to one when ε is super close to zero. We will comment on this phenomenon for the error of the pressure at the end of this section.

The estimate (6.1) does not imply uniform convergence with respect to ε for our new finite element method. However, as a consequence of the theory below, we will obtain an improved estimate of the form

$$|||\boldsymbol{u} - \boldsymbol{u}_h|||_\varepsilon, \|p - p_h\|_0 \leq c \min(h^{1/2}, h\varepsilon^{-1/2}), \tag{6.2}$$

for solutions with a singular behavior similar to the solution $\boldsymbol{u}$ studied here. Note that this is in fact consistent with the results of Tables 6.1 and 6.2, where we never observe a convergence rate below a half. □

The main purpose of this section is to establish error estimates which are uniform with respect to the perturbation parameter ε. We shall show a uniform $O(h^{1/2})$ error estimate in the energy norm. We observe that if $g \in H^1 \cap L_0^2$ then it follows directly from Theorem 5.1 that

$$\| \operatorname{div}(\boldsymbol{u} - \boldsymbol{u}_h)\|_0 \leq c\, h \|g\|_1, \tag{6.3}$$

where the constant c is independent of ε and h. Hence, we have uniform linear convergence for the error of the divergence. In contrast to this, the remaining part of the error will be affected by boundary layers as ε becomes small. However, the following uniform convergence estimate will be derived.

Theorem 6.1. *If $\boldsymbol{f} \in \boldsymbol{H}(\mathrm{rot})$ and $g \in H_+^1$ then there is a constant c, independent of $\boldsymbol{f}$, g, ε, and h such that*

$$\|\boldsymbol{u} - \boldsymbol{u}_h\|_0 + \varepsilon \| \operatorname{rot}(\boldsymbol{u} - \boldsymbol{u}_h)\|_0 + \|p - p_h\|_0 \leq c\, h^{1/2}(\|\boldsymbol{f}\|_{\mathrm{rot}} + \|g\|_{1,+}).$$

Here the Sobolev space H_+^1 is a space contained in H^1, with associated norm, $\|\cdot\|_{1,+}$, slightly stronger than $\|\cdot\|_1$. This space will be precisely defined below.

The derivation of the uniform error estimate above will depend heavily on certain regularity estimates for the solution of the system (1.1). For example, we shall estimate the blow up of $\| \operatorname{rot} \boldsymbol{u}\|_1$ as ε approaches zero. We shall therefore first derive these regularity estimates.

For convenience of the reader we repeat the system (1.1):

$$\begin{aligned} (\boldsymbol{I} - \varepsilon^2 \boldsymbol{\Delta})\boldsymbol{u} - \mathbf{grad}\, p &= \boldsymbol{f} \quad \text{in } \Omega, \\ \operatorname{div} \boldsymbol{u} &= g \quad \text{in } \Omega, \\ \boldsymbol{u} &= 0 \quad \text{on } \partial\Omega. \end{aligned} \tag{6.4}$$

We also repeat that the domain Ω is a polygonal domain in $\mathbb{R}^2$. In fact, in the discussion of this section we shall assume that Ω in addition is *convex*. If $\varepsilon \in (0, 1]$, $\boldsymbol{f} \in \boldsymbol{L}^2$ and $g = 0$ then the corresponding weak solution admits the additional regularity that $(\boldsymbol{u}, p) \in (\boldsymbol{H}_0^1 \times L_0^2) \cap (\boldsymbol{H}^2 \times H^1)$. This regularity result follows directly from the result for the corresponding Stokes problem on a convex domain which can be found in [12, Corollary 7.3.3.5]. In fact, the same regularity holds for $g \neq 0$ if we restrict the data g to the space H_+^1.

In order to define this space let $x_1, x_2, \ldots, x_N \in \partial\Omega$ denote the vertices of Ω. The space H_+^1 is given by

$$H_+^1 = \{g \in H^1 \cap L_0^2 : \int_\Omega \frac{|g(x)|^2}{|x - x_j|^2}\, dx < \infty,\ j = 1, 2, \ldots, N\},$$

with associated norm

$$\|g\|_{1,+}^2 = \|g\|_1^2 + \sum_{j=1}^{N} \int_\Omega \frac{|g(x)|^2}{|x - x_j|^2}\, dx.$$

Hence, functions in H_+^1 vanish weakly at each vertex of Ω.

It is established in [2] that

$$\operatorname{div}(\boldsymbol{H}^2 \cap \boldsymbol{H}_0^1) = H_+^1.$$

Furthermore, the divergence operator has a bounded right inverse, $\boldsymbol{R} : H_+^1 \mapsto \boldsymbol{H}^2 \cap \boldsymbol{H}_0^1$, i.e. $\operatorname{div} \boldsymbol{R}g = g$ for all $g \in H_+^1$ and

$$\|\boldsymbol{R}g\|_2 \leq c\|g\|_{1,+}.$$

Note that if $(\boldsymbol{u}, p)$ solves (6.4) then $(\boldsymbol{u} - \boldsymbol{R}g, p)$ solves a corresponding problem with $g = 0$. From the result in the case $g = 0$ we can therefore conclude that $(\boldsymbol{u}, p) \in (\boldsymbol{H}_0^1 \times L_0^2) \cap (\boldsymbol{H}^2 \times H^1)$ for any $(\boldsymbol{f}, g) \in \boldsymbol{L}^2 \times H_+^1$.

The following result gives an upper bound for the blow up of the norm $\|\operatorname{rot} \boldsymbol{u}\|_1$ as ε tends to zero.

Lemma 6.1. *Assume that $\boldsymbol{f} \in \boldsymbol{H}(\mathrm{rot})$, $g \in H_+^1$, and let $(\boldsymbol{u}, p)$ be the corresponding solution of (6.4). There exist a constant $c > 0$, independent of ε, $\boldsymbol{f}$ and g, such that*

$$\varepsilon^{1/2}\|\operatorname{rot} \boldsymbol{u}\|_0 + \varepsilon^{3/2}\|\operatorname{rot} \boldsymbol{u}\|_1 \leq c\,(\|\operatorname{rot} \boldsymbol{f}\|_0 + \|g\|_{1,+}). \tag{6.5}$$

Proof. We first construct a function $\hat{\boldsymbol{u}} \in \boldsymbol{H}^2 \cap \boldsymbol{H}_0^1$ such that

$$\operatorname{div} \hat{\boldsymbol{u}} = g, \qquad \text{and} \qquad \operatorname{rot} \boldsymbol{\Delta}\hat{\boldsymbol{u}} = 0. \tag{6.6}$$

In fact, the function $\hat{\boldsymbol{u}}$ can be constructed by defining

$$\hat{\boldsymbol{u}} = \boldsymbol{R}g + \mathbf{curl}\, \psi,$$

with $\psi \in H_0^2$ being the weak solution of the biharmonic equation

$$\begin{aligned} \Delta^2 \psi &= \operatorname{rot} \boldsymbol{\Delta} \boldsymbol{R} g \qquad \text{in } \Omega, \\ \psi = \frac{\partial \psi}{\partial \boldsymbol{n}} &= 0 \qquad \text{on } \partial\Omega. \end{aligned}$$

We observe that, since $\boldsymbol{R}g \in \boldsymbol{H}^2$, the right hand side is in H^{-1}. Therefore, from the regularity of solutions of the biharmonic equation on convex domains, cf. [12, Theorem 7.2.2.3], we have that $\psi \in H^3$, and $\|\psi\|_3 \leq c\| \operatorname{rot} \boldsymbol{\Delta} \boldsymbol{R} g\|_{-1}$. Hence, $\hat{\boldsymbol{u}} \in \boldsymbol{H}^2 \cap \boldsymbol{H}_0^1$, and

$$\|\hat{\boldsymbol{u}}\|_2 \leq c \, \|g\|_{1,+}. \tag{6.7}$$

Furthermore, clearly $\operatorname{div} \hat{\boldsymbol{u}} = \operatorname{div} \boldsymbol{R} g = g$, and for any $\mu \in C_0^\infty$ we have

$$(\boldsymbol{\Delta} \hat{\boldsymbol{u}}, \mathbf{curl}\, \mu) = (\boldsymbol{\Delta} \boldsymbol{R} g, \mathbf{curl}\, \mu) - (\Delta \psi, \Delta \mu) = 0.$$

Hence, the second property in (6.6) also holds.

Define $\boldsymbol{v} = \boldsymbol{u} - \hat{\boldsymbol{u}}$. Then $(\boldsymbol{v}, p) \in (\boldsymbol{H}_0^1 \times L_0^2) \cap (\boldsymbol{H}^2 \times H^1)$ is the weak solution of the problem

$$\begin{aligned} (\boldsymbol{I} - \varepsilon^2 \boldsymbol{\Delta}) \boldsymbol{v} - \mathbf{grad}\, p &= \hat{\boldsymbol{f}} \quad \text{in } \Omega, \\ \operatorname{div} \boldsymbol{v} &= 0 \quad \text{in } \Omega, \\ \boldsymbol{v} &= 0 \quad \text{on } \partial\Omega, \end{aligned} \tag{6.8}$$

where $\hat{\boldsymbol{f}} = \boldsymbol{f} + \varepsilon^2 \boldsymbol{\Delta} \hat{\boldsymbol{u}} - \hat{\boldsymbol{u}}$. Clearly, $\hat{\boldsymbol{f}} \in \boldsymbol{L}^2$. In fact, $\hat{\boldsymbol{f}} \in \boldsymbol{H}(\operatorname{rot})$, since

$$\operatorname{rot} \hat{\boldsymbol{f}} = \operatorname{rot} \boldsymbol{f} - \operatorname{rot} \hat{\boldsymbol{u}}.$$

Furthermore, there is a constant c, independent of ε, $\boldsymbol{f}$ and g, such that

$$\| \operatorname{rot} \hat{\boldsymbol{f}}\|_0 \leq c \, (\| \operatorname{rot} \boldsymbol{f}\|_0 + \|g\|_{1,+}). \tag{6.9}$$

Since $\boldsymbol{v} \in \boldsymbol{L}^2$ and $\operatorname{div} \boldsymbol{v} = 0$ there exists $\phi \in H^1$, uniquely determined up to a constant, such that $\boldsymbol{v} = \mathbf{curl}\, \phi$ ([11, Theorem I.3.1]). Hence, since $\boldsymbol{v} \in \boldsymbol{H}^2 \cap \boldsymbol{H}_0^1$, we can choose $\phi \in H^3 \cap H_0^2$. In fact, by applying the rot operator, as a map from $\boldsymbol{L}^2$ to H^{-1}, to the first equation of (6.8) we obtain

$$\begin{aligned} -\Delta \phi + \varepsilon^2 \Delta^2 \phi &= \operatorname{rot} \hat{\boldsymbol{f}} \qquad \text{in } \Omega, \\ \phi = \frac{\partial \phi}{\partial \boldsymbol{n}} &= 0 \qquad \text{on } \partial\Omega. \end{aligned}$$

The function ϕ is uniquely determined by this problem. This singular perturbation problem was in fact studied in [14], where it was established that ([14, Lemma 5.1])

$$\varepsilon^{1/2} \|\phi\|_2 + \varepsilon^{3/2} \|\phi\|_3 \leq c \| \operatorname{rot} \hat{\boldsymbol{f}}\|_0,$$

and as a consequence

$$\varepsilon^{1/2} \| \operatorname{rot} \boldsymbol{v}\|_0 + \varepsilon^{3/2} \| \operatorname{rot} \boldsymbol{v}\|_1 \leq c \| \operatorname{rot} \hat{\boldsymbol{f}}\|_0.$$

Therefore, since $\boldsymbol{u} = \boldsymbol{v} + \hat{\boldsymbol{u}}$, (6.7) and (6.9) implies

$$\begin{aligned}\varepsilon^{1/2}\|\operatorname{rot}\boldsymbol{u}\|_0 + \varepsilon^{3/2}\|\operatorname{rot}\boldsymbol{u}\|_1 &\le c\|\operatorname{rot}\hat{\boldsymbol{f}}\|_0 + \varepsilon^{1/2}(\|\operatorname{rot}\hat{\boldsymbol{u}}\|_0 + \varepsilon\|\operatorname{rot}\hat{\boldsymbol{u}}\|_1)\\ &\le c(\|\operatorname{rot}\boldsymbol{f}\|_0 + \|g\|_{1,+}).\end{aligned}$$

This completes the proof. □

In addition to the ε–dependent bound on the solution $(\boldsymbol{u}, p)$ of (6.4) derived above, we shall also need convergence estimates on how fast these solutions converge to the solution of the reduced system.

The reduced system corresponding to (6.4) is of the form

$$\begin{aligned}\boldsymbol{u}^0 - \mathbf{grad}\, p^0 &= \boldsymbol{f} \quad \text{in } \Omega,\\ \operatorname{div}\boldsymbol{u}^0 &= g \quad \text{in } \Omega,\\ \boldsymbol{u}^0\cdot\boldsymbol{n} &= 0 \quad \text{on } \partial\Omega,\end{aligned} \tag{6.10}$$

A precise weak formulation of this system is given by:

Find $(\boldsymbol{u}^0, p^0) \in \boldsymbol{H}_0(\operatorname{div}) \times L^2_0$ such that

$$\begin{aligned}(\boldsymbol{u}^0, \boldsymbol{v}) + (p^0, \operatorname{div}\boldsymbol{v}) &= (\boldsymbol{f}, \boldsymbol{v}) \qquad \forall \boldsymbol{v} \in \boldsymbol{H}_0(\operatorname{div})\\ (\operatorname{div}\boldsymbol{u}^0, q) &= (g, q) \qquad \forall q \in L^2_0.\end{aligned} \tag{6.11}$$

If $(\boldsymbol{f}, g) \in \boldsymbol{H}^{-1}(\operatorname{rot}) \times L^2_0$ then this system admits a unique solution. In fact, if $\boldsymbol{f} \in \boldsymbol{H}(\operatorname{rot})$ then $\boldsymbol{u}^0 \in \boldsymbol{H}(\operatorname{rot})$ with $\operatorname{rot}\boldsymbol{u}^0 = \operatorname{rot}\boldsymbol{f}$. Therefore,

$$\boldsymbol{u}^0 \in \boldsymbol{H}_0(\operatorname{div}) \cap \boldsymbol{H}(\operatorname{rot}),$$

and hence, cf. [11, Proposition 3.1, Chap. 1], $\boldsymbol{u}^0 \in \boldsymbol{H}^1$. As a consequence, $p^0 \in H^1$. Furthermore, the corresponding solution map is continuous, i.e. there exist a constant c, independent of $\boldsymbol{f}$ and g, such that

$$\|\boldsymbol{u}^0\|_1 + \|p^0\|_1 \le c\,(\|\boldsymbol{f}\|_{\operatorname{rot}} + \|g\|_0). \tag{6.12}$$

Lemma 6.2. *Assume that $\boldsymbol{f} \in \boldsymbol{H}(\operatorname{rot})$, $g \in H^1_+$, and let $(\boldsymbol{u}, p)$ be the corresponding solution of* (6.4). *There exist a constant $c > 0$, independent of ε, $\boldsymbol{f}$ and g, such that*

$$\|\boldsymbol{u} - \boldsymbol{u}^0\|_0 + \|p - p^0\|_1 \le c\,\varepsilon^{1/2}(\|\boldsymbol{f}\|_{\operatorname{rot}} + \|g\|_{1,+}).$$

Proof. It follows from (2.2), the weak formulation of (6.4), and Green's theorem that for any $\boldsymbol{v} \in \boldsymbol{H}^1 \cap \boldsymbol{H}_0(\operatorname{div})$ the solution $(\boldsymbol{u}, p)$ satisfies

$$\begin{aligned}(\boldsymbol{u}, \boldsymbol{v}) + \varepsilon^2(\operatorname{div}\boldsymbol{u}, \operatorname{div}\boldsymbol{v}) + \varepsilon^2(\operatorname{rot}\boldsymbol{u}, \operatorname{rot}\boldsymbol{v}) + \varepsilon^2\int_{\partial\Omega}(\operatorname{rot}\boldsymbol{u})(\boldsymbol{v}\cdot\boldsymbol{t})d\tau\\ + (p, \operatorname{div}\boldsymbol{v}) = (\boldsymbol{f}, \boldsymbol{v}).\end{aligned}$$

By subtracting from this the first equation of (6.11), we obtain

$$(\boldsymbol{u} - \boldsymbol{u}^0, \boldsymbol{v}) + \varepsilon^2(\operatorname{rot}\boldsymbol{u}, \operatorname{rot}\boldsymbol{v}) + \varepsilon^2\int_{\partial\Omega}(\operatorname{rot}\boldsymbol{u})(\boldsymbol{v}\cdot\boldsymbol{t})d\tau = 0$$

for any $\boldsymbol{v} \in \boldsymbol{H}^1 \cap \boldsymbol{H}_0(\mathrm{div})$ with $\mathrm{div}\, \boldsymbol{v} = 0$. Hence, if we take $\boldsymbol{v} = \boldsymbol{u} - \boldsymbol{u}^0$, and observe that $\mathrm{rot}\, \boldsymbol{u}^0 = \mathrm{rot}\, \boldsymbol{f}$ and $\mathrm{div}(\boldsymbol{u} - \boldsymbol{u}^0) = 0$, we derive the identity

$$\|\boldsymbol{u} - \boldsymbol{u}^0\|_0^2 + \varepsilon^2 \|\mathrm{rot}\, \boldsymbol{u}\|_0^2 = \varepsilon^2 \int_{\partial\Omega} (\mathrm{rot}\, \boldsymbol{u})(\boldsymbol{u}^0 \cdot \boldsymbol{t}) d\tau + \varepsilon^2 (\mathrm{rot}\, \boldsymbol{u}, \mathrm{rot}\, \boldsymbol{f}),$$

which immediately leads to the bound

$$\|\boldsymbol{u} - \boldsymbol{u}^0\|_0^2 + \frac{\varepsilon^2}{2} \|\mathrm{rot}\, \boldsymbol{u}\|_0^2 \leq \varepsilon^2 \, \|\mathrm{rot}\, \boldsymbol{f}\|_0^2 + \varepsilon^2 \int_{\partial\Omega} (\mathrm{rot}\, \boldsymbol{u})(\boldsymbol{u}^0 \cdot \boldsymbol{t}) d\tau. \tag{6.13}$$

In order to estimate the boundary integral we note that it follows from Lemma 6.1 and [12, Theorem 1.5.1.10] that

$$\|\mathrm{rot}\, \boldsymbol{u}\|_{0,\partial\Omega} \leq c \|\mathrm{rot}\, \boldsymbol{u}\|_0^{1/2} \|\mathrm{rot}\, \boldsymbol{u}\|_1^{1/2} \leq c\varepsilon^{-1} \, (\|\mathrm{rot}\, \boldsymbol{f}\|_0 + \|g\|_{1,+}).$$

Together with the estimate (6.12) this leads to

$$\begin{aligned} \varepsilon^2 \int_{\partial\Omega} (\mathrm{rot}\, \boldsymbol{u})(\boldsymbol{u}^0 \cdot \boldsymbol{t}) d\tau &\leq \varepsilon^2 \|\mathrm{rot}\, \boldsymbol{u}\|_{0,\partial\Omega} \|\boldsymbol{u}^0\|_1 \\ &\leq c\, \varepsilon (\|\boldsymbol{f}\|_{\mathrm{rot}}^2 + \|g\|_{1,+}^2). \end{aligned}$$

Hence, the estimate

$$\|\boldsymbol{u} - \boldsymbol{u}^0\|_0 + \varepsilon^2 \|\mathrm{rot}\, \boldsymbol{u}\|_0^2 \leq c\, \varepsilon^{1/2} (\|\boldsymbol{f}\|_{\mathrm{rot}} + \|g\|_{1,+}) \tag{6.14}$$

follows.

The estimate for $\|p - p^0\|_1$ is now a direct consequence of the identity

$$\begin{aligned} \mathbf{grad}(p - p^0) &= \boldsymbol{u} - \boldsymbol{u}^0 - \varepsilon^2 \boldsymbol{\Delta} \boldsymbol{u} \\ &= \boldsymbol{u} - \boldsymbol{u}^0 + \varepsilon^2 (\mathbf{curl}\, \mathrm{rot}\, \boldsymbol{u} - \mathbf{grad}\, g) \end{aligned}$$

and the previously established bounds. In fact, it follows from Lemma 6.1 and (6.14) that

$$\begin{aligned} \|\mathbf{grad}(p - p^0)\|_0 &\leq \|\boldsymbol{u} - \boldsymbol{u}^0\|_0 + \varepsilon^2 (\|\mathrm{rot}\, \boldsymbol{u}\|_1 + \|g\|_1) \\ &\leq c\, \varepsilon^{1/2} (\|\boldsymbol{f}\|_{\mathrm{rot}} + \|g\|_{1,+}). \end{aligned}$$

Since $p - p^0 \in L_0^2$, an application of the Poincaré inequality completes the proof. □

The regularity bounds derived above will now be used to prove the uniform convergence estimates.

Proof of Theorem 6.1. Recall that since $\boldsymbol{u} \in \boldsymbol{H}_0^1$ it follows from [11, Proposition 3.1, Chap. 1] that

$$\|\boldsymbol{u}\|_1 \leq c(\|\mathrm{div}\, \boldsymbol{u}\|_0 + \|\mathrm{rot}\, \boldsymbol{u}\|_0).$$

Furthermore, by the standard H^2–regularity for solutions of the Poisson equation on convex domains, and (2.2), we obtain

$$\|\boldsymbol{u}\|_2 \leq c \|\boldsymbol{\Delta} \boldsymbol{u}\|_0 \leq c(\|\mathrm{div}\, \boldsymbol{u}\|_1 + \|\mathrm{rot}\, \boldsymbol{u}\|_1).$$

Hence, from the estimates given in Lemmas 6.1 and 6.2 we conclude that

$$\varepsilon^2\|\boldsymbol{u}\|_2+\varepsilon\|\boldsymbol{u}\|_1+\|\boldsymbol{u}-\boldsymbol{u}^0\|_0+\|p-p^0\|_1 \le c\varepsilon^{1/2}(\|\boldsymbol{f}\|_{\mathrm{rot}}+\|g\|_{1,+}). \tag{6.15}$$

The desired estimate on the velocity error will be derived from (5.4). We will first establish the interpolation estimate

$$\|\boldsymbol{u}-\boldsymbol{\Pi}_h\boldsymbol{u}\|_0+\varepsilon\|\boldsymbol{D}(\boldsymbol{u}-\boldsymbol{\Pi}_h\boldsymbol{u})\|_1 \le c\,h^{1/2}(\|\boldsymbol{f}\|_{\mathrm{rot}}+\|g\|_{1,+}). \tag{6.16}$$

From (4.6), (6.12), and (6.15) we have

$$\begin{aligned}\|\boldsymbol{u}-\boldsymbol{\Pi}_h\boldsymbol{u}\|_0 &\le \|(\boldsymbol{I}-\boldsymbol{\Pi}_h)(\boldsymbol{u}-\boldsymbol{u}^0)\|_0+\|\boldsymbol{u}^0-\boldsymbol{\Pi}_h\boldsymbol{u}^0\|_0\\ &\le ch^{1/2}\left(\|\boldsymbol{u}-\boldsymbol{u}^0\|_0^{1/2}\|\boldsymbol{u}-\boldsymbol{u}^0\|_1^{1/2}+h^{1/2}\,\|\boldsymbol{u}^0\|_1\right)\\ &\le ch^{1/2}(\|\boldsymbol{f}\|_{\mathrm{rot}}+\|g\|_{1,+}).\end{aligned}$$

Furthermore, from (4.4), (4.5), and (6.15),

$$\begin{aligned}\varepsilon\|\boldsymbol{D}(\boldsymbol{u}-\boldsymbol{\Pi}_h\boldsymbol{u})\|_0 \le c\varepsilon\|\boldsymbol{u}\|_1^{1/2}\|\boldsymbol{u}-\boldsymbol{\Pi}_h\boldsymbol{u}\|_1^{1/2} &\le c\varepsilon h^{1/2}\|\boldsymbol{u}\|_1^{1/2}\|\boldsymbol{u}\|_2^{1/2}\\ &\le ch^{1/2}(\|\boldsymbol{f}\|_{\mathrm{rot}}+\|g\|_{1,+}).\end{aligned}$$

The estimate (6.16) is therefore verified.

Similarly, since $\|\boldsymbol{u}\|_1^{1/2}\|\boldsymbol{u}\|_2^{1/2} \le c\varepsilon^{-1}(\|\boldsymbol{f}\|_{\mathrm{rot}}+\|g\|_{1,+})$, we obtain from Lemma 5.1 that

$$\sup_{\boldsymbol{v}\in\boldsymbol{V}_h}\frac{|E_{\varepsilon,h}(\boldsymbol{u},\boldsymbol{v})|}{\|\boldsymbol{v}\|_a} \le ch^{1/2}(\|\boldsymbol{f}\|_{\mathrm{rot}}+\|g\|_{1,+}). \tag{6.17}$$

However, by combining (5.4), (6.3), (6.16), and (6.17), this implies

$$\|\boldsymbol{u}-\boldsymbol{u}_h\|_0+\varepsilon\|\operatorname{rot}(\boldsymbol{u}-\boldsymbol{u}_h)\|_0 \le ch^{1/2}(\|\boldsymbol{f}\|_{\mathrm{rot}}+\|g\|_{1,+}). \tag{6.18}$$

In order to establish the estimate for the $\|p-p_h\|_0$ note that (4.3) and (6.15) implies

$$\|P_hp-p\|_0 \le ch\|p\|_1 \le ch(\|\boldsymbol{f}\|_{\mathrm{rot}}+\|g\|_{1,+}).$$

Finally, by (5.6), (6.17), and (6.18),

$$\|P_hp-p_h\|_0 \le ch^{1/2}(\|\boldsymbol{f}\|_{\mathrm{rot}}+\|g\|_{1,+}).$$

This completes the proof of Theorem 6.1. □

Remark. Even if Lemma 6.2 states that $\|p\|_1$ is uniformly bounded with respect to ε, we are not able to prove that $\|p-p_h\|_0$ converges linearly in h uniformly in ε. The convergence rate is polluted by the blow up of $\boldsymbol{u}$. This seem to agree with what we observed in Example 6.1 above, cf. Table 6.2. □

7. An associated elliptic system

In this section we shall study the elliptic system (1.2) given by

$$
\begin{aligned}
(\boldsymbol{I} - \varepsilon^2 \boldsymbol{\Delta})\boldsymbol{u} - \delta^{-2}\,\mathbf{grad}(\operatorname{div} \boldsymbol{u} - g) &= \boldsymbol{f} \quad \text{in } \Omega, \\
\boldsymbol{u} &= 0 \quad \text{on } \partial\Omega,
\end{aligned} \tag{7.1}
$$

where $\varepsilon, \delta \in (0, 1]$. Recall that by introducing $p = \delta^{-2} \operatorname{div} \boldsymbol{u}$ this system can be alternatively be written on the mixed form (1.3). Hence, as δ approach zero the system formally reduces to (1.1).

The system (7.1) will be discretized by a standard finite element approach, i.e. the mixed system (1.3) is not introduced in the discretization. Let the bilinear form $b_{\varepsilon,\delta}(\cdot,\cdot)$ be defined by

$$
\begin{aligned}
b_{\varepsilon,\delta}(\boldsymbol{u}, \boldsymbol{v}) &= a_\varepsilon(\boldsymbol{u}, \boldsymbol{v}) + \delta^{-2}(\operatorname{div} \boldsymbol{u}, \operatorname{div} \boldsymbol{v}) \\
&= (\boldsymbol{u}, \boldsymbol{v}) + \varepsilon^2(\boldsymbol{D}\boldsymbol{u}, \boldsymbol{D}\boldsymbol{v}) + \delta^{-2}(\operatorname{div} \boldsymbol{u}, \operatorname{div} \boldsymbol{v}).
\end{aligned}
$$

For a given finite element space $\boldsymbol{V}_h$, the corresponding standard finite element discretization of (7.1) is given by:

Find a $\boldsymbol{u}_h \in \boldsymbol{V}_h$ such that

$$
b_{\varepsilon,\delta}(\boldsymbol{u}_h, \boldsymbol{v}) = (\boldsymbol{f}, \boldsymbol{v}) + \delta^{-2}(g, \operatorname{div} \boldsymbol{v}) \qquad \forall \boldsymbol{v} \in \boldsymbol{V}_h. \tag{7.2}
$$

Our purpose here is to discuss this discretization when the finite element space $\boldsymbol{V}_h$ is the space introduced in §4 above. Since this space is not a subspace of $\boldsymbol{H}_0^1$ this will lead to a nonconforming discretization of the system (7.1). However, before we analyze this discretization, we will present some numerical experiments based on the system (7.1).

Example 7.1 In all the examples presented in this section we consider the system (7.1) with $\boldsymbol{u} = \mathbf{curl} \sin^2(\pi x_1) \sin^2(\pi x_2)$, $g = 0$, and $\boldsymbol{f} = \boldsymbol{u} - \varepsilon^2 \boldsymbol{\Delta} \boldsymbol{u}$. Hence, the solution is independent of ε and δ.

We consider the problem (7.1) with Ω taken as the unit square. The domain is triangulated as described in Example 3.1. The system is then discretized by solving the system (7.2), where the space $\boldsymbol{V}_h$ is the standard space of continuous piecewise linear functions with respect to this triangulation.

In the present example we have used $\varepsilon = 1$, while δ and h varies. In Table 7.1 below we have computed the relative error in the L^2 norm for different values of δ and h.

$\delta \backslash h$	2^{-2}	2^{-3}	2^{-4}	2^{-5}	2^{-6}	rate
1.00	3.87e-1	1.32e-1	3.69e-2	9.52e-3	2.39e-3	1.85
0.10	9.19e-1	7.28e-1	4.34e-1	1.88e-1	6.20e-2	0.97
0.01	1.00	9.96e-1	9.82e-1	9.32e-1	7.88e-1	0.08

Table 7.1. The relative L^2 error using piecewise linear elements, $\varepsilon = 1$.

As expected we observe approximately quadratic convergence with respect to h for $\delta = 1$. However the convergence clearly deteriorates as δ tends to zero. □

Example 7.2 We repeat the experiment above, but we extend the finite element space and use the corresponding velocity space of the Mini element instead of the piecewise linear space. It is interesting to note that the L^2 convergence deteriorates, as δ gets small, also in this case, in contrast to what we have observed in Table 3.7. The relative L^2 error is given in Table 7.2.

$\delta\backslash h$	2^{-2}	2^{-3}	2^{-4}	2^{-5}	2^{-6}	rate
1.00	3.80e-1	1.30e-1	3.62e-2	9.34e-3	2.35e-3	1.85
0.10	9.19e-1	7.28e-1	4.34e-1	1.88e-1	6.20e-2	0.97
0.01	9.99e-1	9.96e-1	9.82e-1	9.33e-1	7.88e-1	0.08

TABLE 7.2. The relative L^2 error using the Mini element, $\varepsilon = 1$.

We observe that the results are almost identical to the ones we obtained in the piecewise linear case. Hence, the extra bubble functions have almost no effect. Of course, the main reason for the difference between the results given here, for δ small, and the results given in Example 3.3, where $\delta = 0$, is that the second equation of the mixed method used previously implicitly introduces a reduced integration in the divergence term. □

Example 7.3 We repeat the experiment above once more, but this time we use the new nonconforming element. In Table 7.3 below we have computed the relative error in the energy norm, i.e. the norm generated by the form $b_{\varepsilon,\delta}$, for different values of δ and h.

$\delta\backslash h$	2^{-2}	2^{-3}	2^{-4}	2^{-5}	2^{-6}	rate
1.00	1.84	9.83e-1	4.98e-1	2.50e-1	1.25e-1	0.97
0.10	1.83	9.66e-1	4.87e-1	2.44e-1	1.22e-1	0.98
0.01	1.83	9.66e-1	4.87e-1	2.44e-1	1.22e-1	0.98

TABLE 7.3. The relative error in energy norm for the new nonconforming element, $\varepsilon = 1$.

In contrast to the other examples above, in this case the convergence seems to be linear with respect to h, uniformly in δ. We also observe that the errors are almost independent of δ.

Next, we reduce ε and take $\varepsilon = 0.01$ and redo the experiment. The results are given in Table 7.4.

We observe that to the given accuracy, the numerical solution is independent of δ, clearly indicating that the numerical solutions are

$\delta\backslash h$	2^{-2}	2^{-3}	2^{-4}	2^{-5}	2^{-6}	rate
1.00	1.04e-1	3.23e-2	8.94e-3	2.21e-3	5.29e-4	1.91
0.10	1.04e-1	3.23e-2	8.94e-3	2.21e-3	5.29e-4	1.91
0.01	1.04e-1	3.23e-2	8.94e-3	2.21e-3	5.29e-4	1.91

TABLE 7.4. The relative error in energy norm for the new nonconforming element, $\varepsilon = 0.01$.

close to a pure curl field independent of δ, which is precisely the form of the exact solution in this case. A similar observation is done if we take $\varepsilon = 0$. □

The numerical experiments just presented indicate that the nonconforming space $\boldsymbol{V}_h$, introduced in §4 above, is well suited for the problem (7.1). We will give a partial theoretical justification for this claim by deriving a generalization of Theorem 5.1.

We assume throughout this section that $\boldsymbol{u} \in \boldsymbol{H}^2 \cap \boldsymbol{H}_0^1$. Let $\|\cdot\|_b$ be the energy norm associated with the system (7.1), i.e.

$$\|\boldsymbol{v}\|_b^2 = b_{\varepsilon,\delta}(\boldsymbol{v}, \boldsymbol{v}).$$

It is a straightforward consequence of the second Strang lemma, cf. [9, Theorem 4.2.2], that there exists a $c > 0$ independent of ε, h and $\boldsymbol{u}$ such that

$$\|\boldsymbol{u} - \boldsymbol{u}_h\|_b^2 \leq \|\boldsymbol{u} - \boldsymbol{\Pi}_h \boldsymbol{u}\|_b^2 + c \sup_{\boldsymbol{v} \in \boldsymbol{V}_h} \frac{|E_{\varepsilon,h}(\boldsymbol{u}, \boldsymbol{v})|^2}{\|\boldsymbol{v}\|_b^2}, \tag{7.3}$$

where the inconsistency error $E_{\varepsilon,h}$ is introduced in §5 above. However, since $\|\boldsymbol{v}\|_b \geq \|\boldsymbol{v}\|_a$, the inconsistency term can be bounded as in Lemma 5.1. Furthermore, (4.5) implies

$$\|\boldsymbol{u} - \boldsymbol{\Pi}_h \boldsymbol{u}\|_a \leq c(h^2 + \varepsilon h)\|\boldsymbol{u}\|_2.$$

As a consequence of the fact that $\operatorname{div} \boldsymbol{\Pi}_h \boldsymbol{u} = P_h \operatorname{div} \boldsymbol{u}$, it is also true that

$$\|\operatorname{div}(\boldsymbol{u} - \boldsymbol{u}_h)\|_0^2 = \|\operatorname{div}(\boldsymbol{u} - \boldsymbol{\Pi}_h \boldsymbol{u})\|_0^2 + \|\operatorname{div}(\boldsymbol{\Pi}_h \boldsymbol{u} - \boldsymbol{u}_h)\|_0^2.$$

Thus, we can conclude from (7.3) that

$$\begin{aligned} \|\boldsymbol{u} - \boldsymbol{u}_h\|_a^2 + \delta^{-2}\|(I - P_h)\operatorname{div} \boldsymbol{u}\|_0^2 + \delta^{-2}\|\operatorname{div}(\boldsymbol{\Pi}_h \boldsymbol{u} - \boldsymbol{u}_h)\|_0^2 \\ \leq c(h^2 + \varepsilon h)^2 \|\boldsymbol{u}\|_2^2 + \delta^{-2}\|(I - P_h)\operatorname{div} \boldsymbol{u}\|_0^2. \end{aligned}$$

We therefore have established the following convergence result.

Theorem 7.1. *If $\boldsymbol{u} \in \boldsymbol{H}^2 \cap \boldsymbol{H}_0^1$ then*

$$\|\boldsymbol{u} - \boldsymbol{u}_h\|_0 + \varepsilon\|\operatorname{rot}(\boldsymbol{u} - \boldsymbol{u}_h)\|_0 + \delta^{-1}\|\operatorname{div}(\boldsymbol{\Pi}_h \boldsymbol{u} - \boldsymbol{u}_h)\|_0 \leq c(h^2 + \varepsilon h)\|\boldsymbol{u}\|_2.$$

Here $c > 0$ is a constant independent of ε, δ and h.

Note that from this result we can conclude that if ε and h are fixed, and δ approaches zero, then $\operatorname{div} \boldsymbol{u}_h$ converges in L^2 to $P_h \operatorname{div} \boldsymbol{u}$. Furthermore, the divergence of the error can be controlled by this estimate since

$$\begin{aligned}\|\operatorname{div}(\boldsymbol{u} - \boldsymbol{u}_h)\|_0 &\leq \|(I - P_h)\operatorname{div} \boldsymbol{u}\|_0 + \|\operatorname{div}(\boldsymbol{\Pi}_h \boldsymbol{u} - \boldsymbol{u}_h)\|_0 \\ &\leq ch\|\operatorname{div} \boldsymbol{u}\|_1 + c\delta(\varepsilon^2 + h\varepsilon)\|\boldsymbol{u}\|_2.\end{aligned}$$

Of course, exactly as for the problem (1.1) we can argue that, in general cases, the norm $\|\boldsymbol{u}\|_2$ will not remain bounded as ε and δ approach zero. Hence, ideally we would like to generalize the results of §6 to the problem (7.1). However, this discussion is outside the scope of this paper.

Acknowledgment. The authors are grateful to Professors D.N Arnold, R.S. Falk and Z. Cai for many useful discussions.

References

[1] D.N. Arnold, F. Brezzi and M. Fortin, A stable finite element method for the Stokes equations, Calcolo 21 (1984), pp. 337–344.
[2] D.N. Arnold, L.R. Scott and M. Vogelius, Regular inversion of the divergence operator with Dirichlet boundary conditions on a polygon, Ann. Scuola Norm. Sup. Pisa Cl. Sci.–Serie IV **XV** (1988), pp. 169–192.
[3] J.H. Bramble and J.E. Pasciak, Iterative techniques for time dependent Stokes problem, Comput. Math. Appl. 33 (1997), pp. 13–30.
[4] J. Bergh and J. Löfström, *Interpolation spaces*, Springer Verlag, 1976.
[5] S.C. Brenner and L.R. Scott, *The mathematical theory of finite element methods*, Springer Verlag, 1994.
[6] F. Brezzi, On the existence, uniqueness and approximation of saddle–point problems arising from Lagrangian multipliers, RAIRO Anal. Numér. 8 (1974), pp. 129–151.
[7] F. Brezzi, J. Douglas and L.D. Marini, Two families of mixed finite elements for second order elliptic problems, Numer. Math. 47 (1985), pp. 217–235.
[8] F. Brezzi and M. Fortin, *Mixed and hybrid finite element methods*, Springer Verlag, 1991.
[9] P.G. Ciarlet, *The finite element method for elliptic problems,* North–Holland Publishing Company, 1978.
[10] M. Crouzeix and P.A. Raviart, Conforming and non–conforming finite element methods for solving the stationary Stokes equations, RAIRO Anal. Numér. 7 (1973), pp. 33–76.
[11] V. Girault and P.-A. Raviart, *Finite element methods for Navier–Stokes equations*, Springer Verlag 1986.
[12] P. Grisvard, *Elliptic problems on nonsmooth domains,* Monographs and studies in mathematics vol. 24, Pitman Publishing Inc., 1985.
[13] E. Haug, T. Rusten and H. Thevik, A mathematical model for macrosegregationformation in binary alloy solidification, in *Numerical methods and software tools in industial mathematics,* M. Dæhlen and A. Tveito eds., Birkhäuser, 1997.
[14] T.K. Nilssen, X-C Tai and R. Winther, A robust nonconforming H^2–element, Math. Comp. 70 (2000), pp. 489–505.

[15] P.A. Raviart and J.M. Thomas, A mixed finite element method for second order elliptic problems, *Mathematical aspects of finite element methods*, Lecture Notes in Mathematics 606, Springer–Verlag 1977.
[16] S. Whitaker, Flow in porous media I: A theoretical derivation of Darcy's law, Transport in porous media 1 (1986), pp. 3–25.
[17] O.C. Zienkiewicz and R.L. Taylor, The Finite Element Method, Butterworth-Heinemann, 2000.

Department of Informatics, University of Oslo, P.O. Box 1080 Blindern, 0316 Oslo, Norway
E-mail address: kent-and@ifi.uio.no

Department of Mathematics, University of Bergen, Johannes Brunsgt. 12, 5007 Bergen, Norway
E-mail address: Xue-Cheng.Tai@mi.uib.no

Department of Informatics and Department of Mathematics, University of Oslo, P.O. Box 1080 Blindern, 0316 Oslo, Norway
E-mail address: rwinther@ifi.uio.no